Chapter 2
Hot Big Bang Model

This to attain, whether heav'n move or earth,
Imports not, if thou reckon right; the rest
From man or angel the great Architect
Did wisely to conceal, and not divulge
His secrets to be scanned by them who aught
Rather admire; or if they list to try
Conjecture, he his fabric of the heav'ns
Hath left to their disputes, perhaps to move
His laughter at their quaint opinions wide
Hereafter, when they come to model heav'n
And calculate the stars ...

— Milton, *Paradise Lost,* VIII, 70–80

Contents

G. Calcagni, *Classical and Quantum Cosmology*, Graduate Texts in Physics,
DOI 10.1007/978-3-319-41127-9_2

2.1 Cosmic Expansion and Cosmological Principle

2.1.1 The Universe at Large Scales

Cosmology is the study of Nature at very large scales. Conventionally, "large scales" span a range of about 1–8000 Mpc, from our local group of galaxies to the most distant light we can possibly detect (Fig. 2.1). Phenomena occurring within a galaxy (ours or another) and associated with galactic media, stars, supernovæ, black holes, gamma-ray bursts and so on are also part of cosmology, in so far as they determine relative distances, ages, composition and gravitational properties of local patches of the universe, as well as important information on elementary particle physics and gravity.

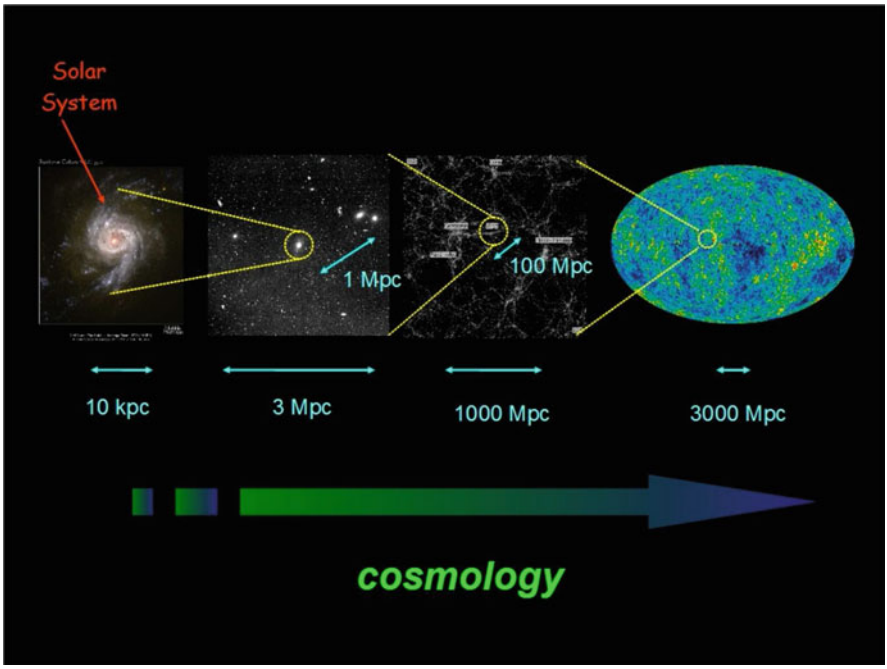

Fig. 2.1 Cosmological scales (Source: adaptation of a figure by C. Schimd)

The large-scale structure of the universe has been studied by several experiments, including the 2-degree Field Galaxy Redshift Survey (2dFGRS) [1], the 6-degree Field Galaxy Survey (6dFGS) [2, 3] and the Sloan Digital Sky Survey (SDSS) [4, 5], later combined with the Supernova Legacy Survey (SNLS) [6, 7]. The first mapped about 4 % of the sky, recording over 220,000 galaxies and 100 quasars as far away as 800 Mpc (see Problem 2.7). The 6dFGS covered a fraction of the sky ten times larger, sampling 125,000 galaxies. The database of the SDSS-III survey covers about one quarter of the sky, over 1,800,000 galaxies and over 300,000 quasars.

The galaxy distribution near the local group is rather irregular and characterized by several super-clusters of galaxies where visible matter is much more concentrated than in other almost-empty regions called giant vacua (Figs. 2.2 and 2.3). However, at larger scales the galaxy distribution becomes more uniform in all directions (Fig. 2.4). With good approximation, the large-scale matter distribution of the universe is *homogeneous* (independent of the point at which the observation takes place) and *isotropic* (independent of the direction of observation). This is all the more apparent at even larger scales. In fact, the sky is also uniformly filled with a radiation background of cosmic origin, called *cosmic microwave background* (CMB). Its distribution has been mapped with great accuracy by the Wilkinson Microwave Anisotropy Probe (WMAP) [10–12] and by the PLANCK satellite [13, 14], and it shows a remarkable degree of isotropy (Fig. 2.5).

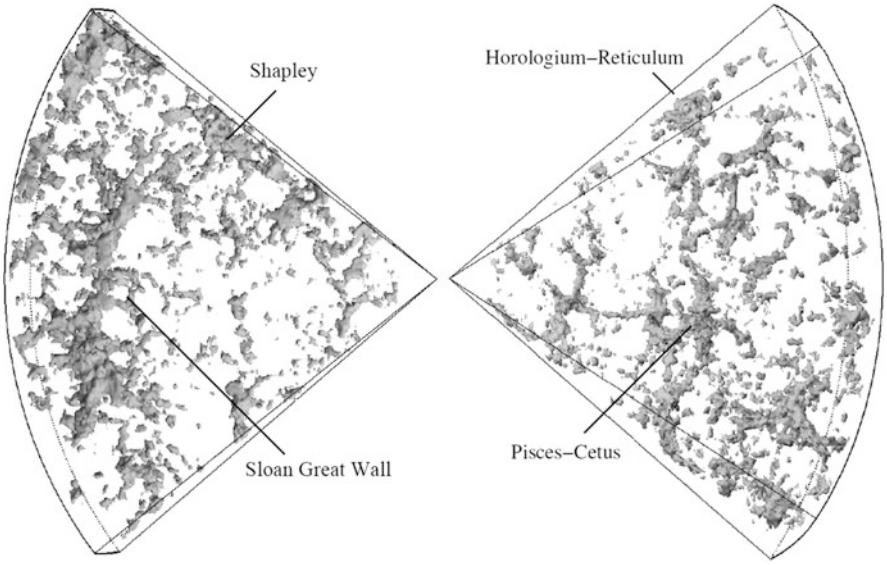

Fig. 2.2 The Sloan Great Wall in a DTFE reconstruction of the inner parts of the 2dF Galaxy Redshift Survey. The most distant galaxies in the figure are at about one billion light years (∼300 Mpc) from Earth (Source: [8])

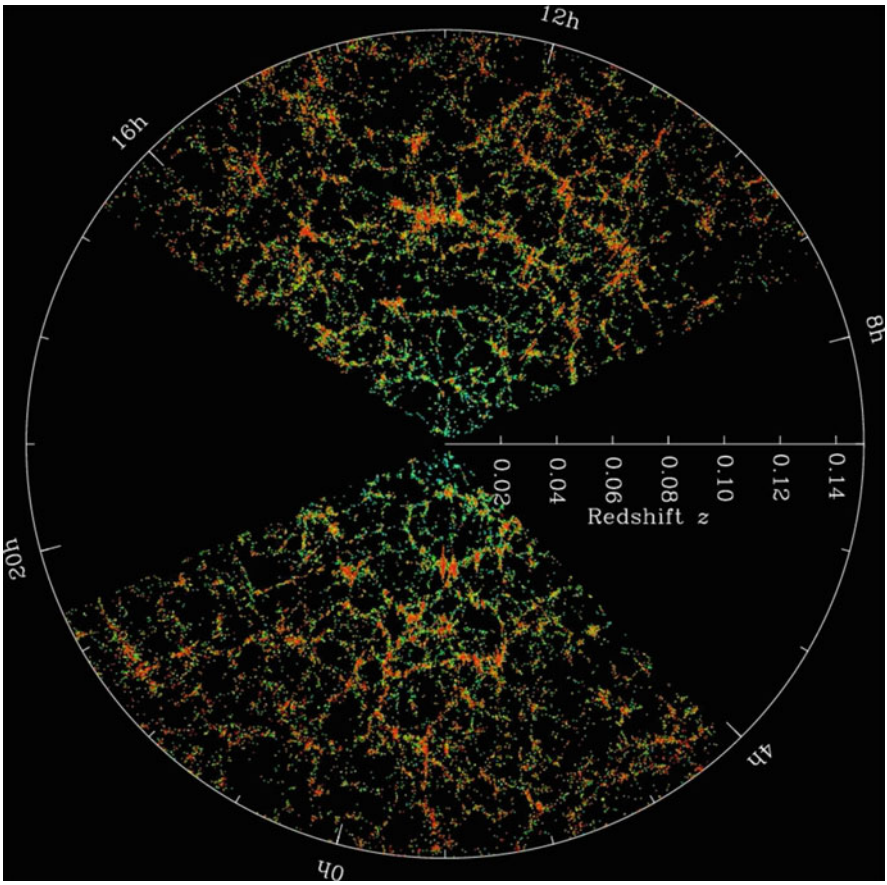

Fig. 2.3 Slices through the SDSS 3-dimensional map of the distribution of galaxies. Earth is at the centre and each point represents a galaxy, typically containing about 100 billion stars. Galaxies are colored according to the ages of their stars, with the redder, more strongly clustered points showing galaxies that are made of older stars. The outer circle is at a distance of two billion light years. The region between the wedges was not mapped by the SDSS because dust in our own Galaxy obscures the view of the distant universe in these directions (Credit: M. Blanton and the Sloan Digital Sky Survey [4])

The CMB is regarded as a snapshot of the universe dated back to more than 13 billion years ago, when matter, a hot homogeneous plasma of baryons and other particles, became transparent to radiation for the first time. Today, the CMB has cooled down to a mean temperature of [15, 16]

$$T_0 = (2.7255 \pm 0.0006)\,\mathrm{K}\,. \tag{2.1}$$

Looking in any direction, the observer measures the same value (isotropy). Since there is no reason why we should occupy a privileged place in the universe, the

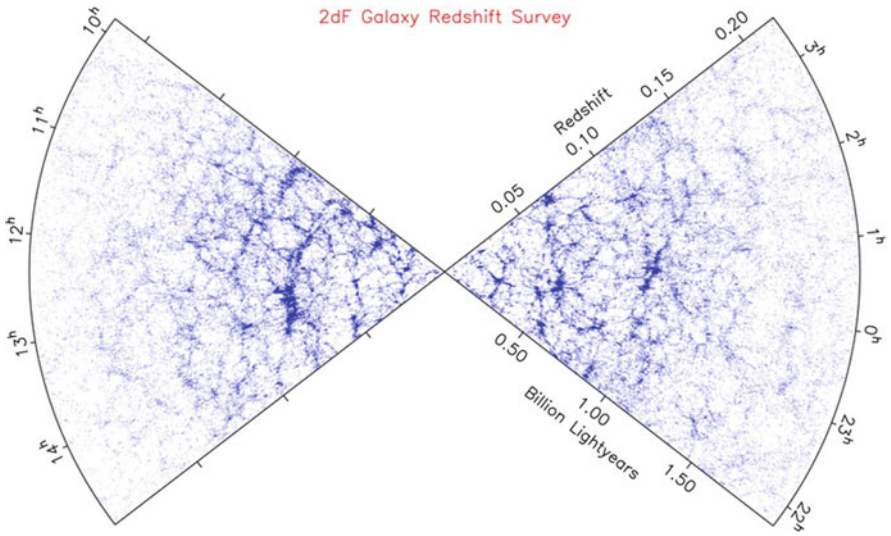

Fig. 2.4 2dFGRS Galaxy map (Credit: 2dF Galaxy Redshift Survey [9])

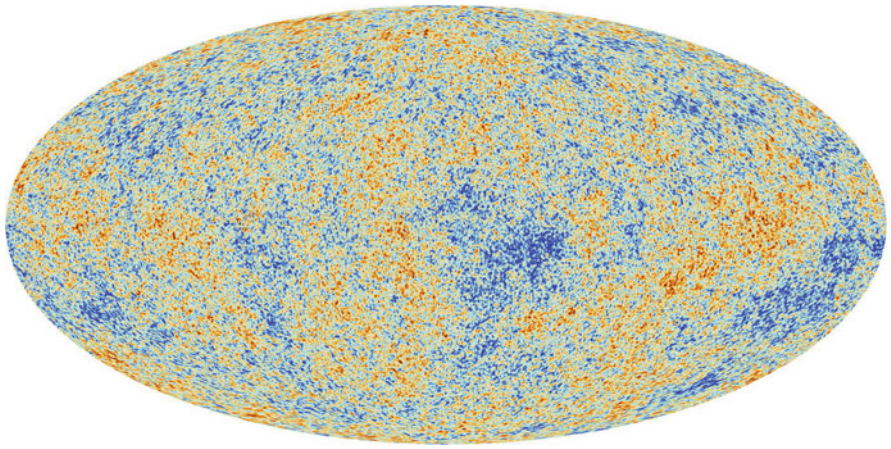

Fig. 2.5 Temperature anisotropy map of the cosmic microwave background radiation in the 2013 PLANCK data release. Colors indicate warmer (*red*) and cooler (*blue*) spots with respect to the mean temperature (©ESA and the Planck Collaboration [13])

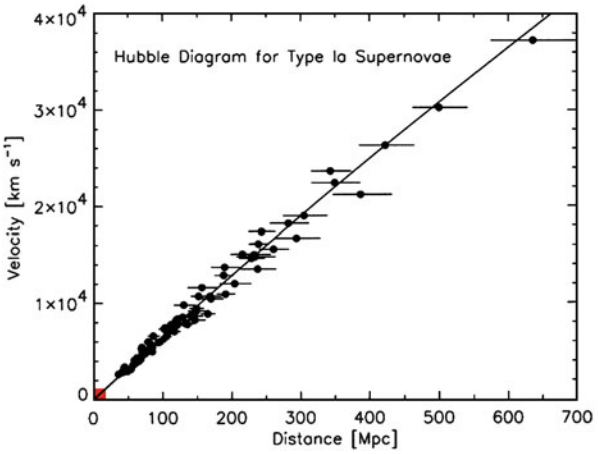

Fig. 2.6 Hubble diagram: recession velocity of extragalactic supernovæ as a function of distance. ©2004 National Academy of Sciences, USA (Source: [17])

same value should be measured also by observers positioned at any other point (homogeneity). Deviations from T_0 are of the order of micro-Kelvins, so that the very distant (i.e., early) universe is, for any observer, homogeneous and isotropic up to one part over 10^5.

We also see other large-scale phenomena. The rotation curves of galaxies and gravitational lensing effects strongly indicate the presence of more matter than what we observe. Baryons and leptons are typically interested by electromagnetic interactions, so that this extra component (called *dark matter*) is believed to be made of exotic particles not yet detected in the laboratory.

Finally, galaxies are seen to recede away from us according to Hubble's law. This law states that the farther the galaxy, the greater the recession speed (Fig. 2.6).[1] Observations of type Ia supernovæ (SNe Ia) show a deviation from the linear Hubble law [18–23], thus indicating that the universe not only expands, but it does so with increasing rate.

To summarize, observations establish the ingredients of the cosmological standard model known, for reasons which shall soon become clear, as *hot big bang* (henceforth "standard model;" we shall use capital initials for the Standard Model of particles):

(I) At sufficiently large scales, the universe is isotropic: its properties are independent of the direction of observation.

(II) Copernican principle: our location is not special. Consequently, if the universe is observed as isotropic from everywhere, it is also homogeneous: its thermal

[1]The distance of a galaxy is determined by astrophysics standard candles such as variable stars and supernovæ. For a historical introduction on Hubble law, see [17].

properties are the same at every point. By "point" we mean a sufficiently large local patch.

(III) The universe is composed of radiation and baryonic as well as non-baryonic matter. At early times, it was in thermal equilibrium.

(IV) The universe expands. At late times, the expansion is accelerated.

Points **(I)** and **(II)** go under the name of cosmological principle:

Cosmological principle. *The universe does not possess a privileged point or direction; it is therefore homogeneous and isotropic (approximately).*

2.1.2 Friedmann–Lemaître–Robertson–Walker Background

The above ingredients can be formalized in Einstein's theory of general relativity. We assume spacetime is a "globally hyperbolic" Lorentzian manifold $(\mathcal{M}, g)$ endowed with a metric $g_{\mu\nu}$. Definitions of global hyperbolicity, space- and time-like curves and geodesics will be given later in the technical Sect. 6.1.1. Here, we only need to grasp the intuitive meaning of global hyperbolicity, namely, the possibility to foliate spacetime into spatial sections stacked along a natural time direction.

Homogeneity and isotropy are realized by the Friedmann–Lemaître–Robertson–Walker (FLRW) metric:

$$\mathrm{d}s^2 = g_{\mu\nu}\mathrm{d}x^\mu \mathrm{d}x^\nu = -\mathrm{d}t^2 + a^2(t)\gamma_{\alpha\beta}\mathrm{d}x^\alpha \mathrm{d}x^\beta \,, \tag{2.2a}$$

where $t = x^0$ is *synchronous* (or *proper*) *time*, $a(t)$ is the expansion parameter or *scale factor*, and

$$\gamma_{\alpha\beta}\mathrm{d}x^\alpha \mathrm{d}x^\beta = \frac{\mathrm{d}r^2}{1 - \mathrm{K}\, r^2} + r^2 \mathrm{d}\Omega_{D-2}^2 \tag{2.2b}$$

is the line element, in hyperspherical coordinates, of the maximally symmetric $(D-1)$-dimensional space $\tilde{\Sigma}$ of constant sectional curvature K (intrinsic curvature). The latter is equal to -1 for an open universe, 0 for a flat universe and $+1$ for a closed universe with radius a (Fig. 2.7). In four dimensions (polar coordinates), $\mathrm{d}\Omega_2^2 = \mathrm{d}\theta^2 + \sin^2\theta \mathrm{d}\varphi^2$, where $0 \leqslant \theta \leqslant \pi$ and $0 \leqslant \varphi \leqslant 2\pi$.

The fact that the universe follows a homogeneous evolution allows us to use the same *universal clock* at each point, so that physical properties which are equal in different places imply synchronized clocks.[2] Sometimes, the choice of a coordinate system (equivalently, of a metric $g_{\mu\nu}$) is referred to as a *gauge* choice. The FLRW

[2]This is true, of course, for large-scale observations, while at very small scales, where non-FLRW metrics are better descriptions of the environment, the problem of synchronization of clocks persists.

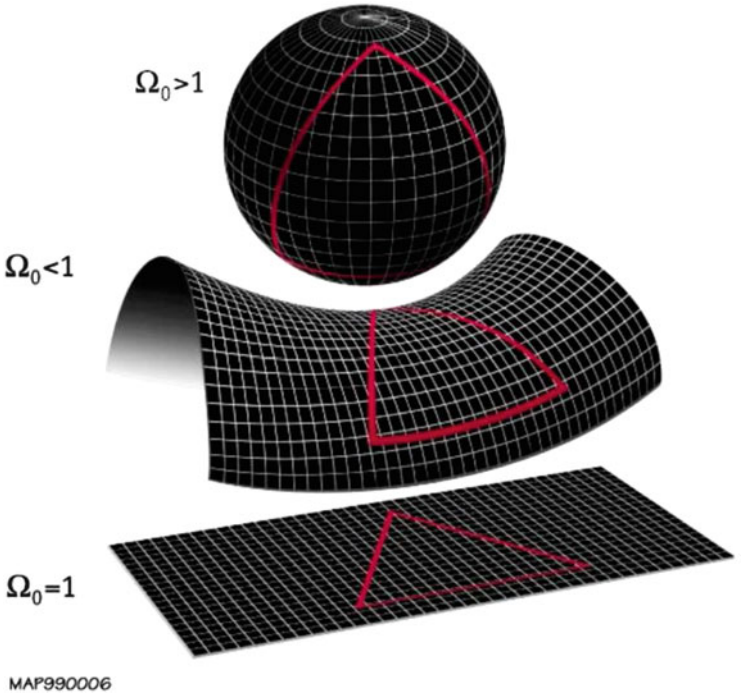

Fig. 2.7 Three possible geometries of the universe illustrated for *two-dimensional* spatial sections: closed, open and flat from top to bottom, corresponding to a total density parameter Ω_0 today respectively greater than, less than or equal to 1 (see (2.84)). In a closed or open $(2+1)$-dimensional universe, the sum of the internal angles of a triangle is, respectively, greater than or less than π. Only in a universe with flat spatial curvature the sum is π (Credit: NASA/WMAP Science Team [10])

metric corresponds to synchronous gauge, which we will meet again later. Another gauge makes use of *conformal time* τ, defined as

$$\mathrm{d}\tau := \frac{\mathrm{d}t}{a(t)}\,. \tag{2.3}$$

The line element (2.2) becomes

$$\mathrm{d}s^2 = a^2(\tau)(-\mathrm{d}\tau^2 + \gamma_{\alpha\beta}\mathrm{d}x^\alpha \mathrm{d}x^\beta)\,.$$

For a free particle moving at the speed of light, the coordinate distance spanned in a conformal time interval $\Delta\tau$ is $c\Delta\tau$.

Since the time coordinate is not physical time, we can choose different universal clocks according to the problem at hand. Apart from t, τ, or the redshift z below, one can also use matter as relational time, provided it evolves monotonically.

For instance, in the presence of a classical scalar field one can make a time reparametrization whenever $\dot{\phi}$ (dots denote differentiation with respect to synchronous time t) does not change sign (non-singular Jacobian), so that the Hubble parameter and other geometrical quantities are thought of as depending on ϕ.

The spatial part of the metric is homogeneous and isotropic by construction. The coordinates x^α are "glued" to the continuous fluid elements representing the matter content. Therefore, a coordinate point x^α in space represents a fluid element passing at time t on the given point. This is why spatial coordinates are called *comoving*. It is easy to relate comoving distances with *proper* distances:

$$\boxed{\text{(proper distance)} = a(t) \times \text{(comoving distance)}\,.} \tag{2.4}$$

Proper distances are also called dynamical or, more often, physical, but we will not use these alternative names here (strictly speaking, comoving distances are also physical and dynamical).

Observations tell us that the universe is expanding, so we assume that the scale factor $a(t) > 0$ increases, $\dot{a}(t) > 0$. Cosmological distances (see Problem 2.7) are better characterized by the *redshift*

$$1 + z := \frac{a_0}{a}\,, \tag{2.5}$$

where $a_0 := a(t_0)$ is the scale factor today. The scale factor is not a physical observable and its normalization is arbitrary. Typically, one chooses $a_0 = 1$. A local observer O is at $z = 0$ and distant objects are at $z > 0$. For large redshift, $1/z$ roughly indicates the size of a closed universe with respect to its radius today.

The name redshift comes from the fact that

$$z = \frac{\lambda_0 - \lambda}{\lambda}\,,$$

where λ is the wave-length of radiation emitted by a source and λ_0 is the observed wave-length. To show this, consider two nearby objects separated by a small proper distance $\mathrm{d}R$, where $\mathrm{d}R = a(1 - \kappa r^2)^{-1/2}\mathrm{d}r$. The relative velocity of the two objects is given by the Hubble law, $\mathrm{d}v = H\mathrm{d}R$. By Doppler law, the infinitesimal change in wave-length is $\mathrm{d}\lambda/\lambda = \mathrm{d}v/c = H\mathrm{d}t = \mathrm{d}a/a$, where we used $c = \dot{R}$. Integrating, we get

$$\frac{\lambda}{a} = \frac{\lambda_0}{a_0}. \tag{2.6}$$

The momentum of a photon scales as a^{-1} or, in other words, the comoving wavelength of the signal is the same at the source and for the observer.

Comoving coordinates define a frame where the universe is isotropic and all observers move along the Hubble flow. On the other hand, a proper observer sees nearby galaxies receding but this does not mean that O is the "centre" of the universe, since there is no privileged point. Redshift measurements and distance statements such as (2.4) always refer to the relative position of the observed object with respect to O. To use a simple analogy, one can imagine the two-dimensional surface of a balloon (the universe) dotted with spots (galaxies). As long as the balloon inflates, the distance between the spots, measured on the balloon surface by a two-dimensional observer, increases.

The *Hubble parameter*

$$H(t) := \frac{\dot{a}(t)}{a(t)} \tag{2.7}$$

describes the expansion rate of the universe and defines the *Hubble distance* (or *radius* or, improperly, *horizon*; c units temporarily restored)

$$R_H(t) := \frac{c}{H(t)}\,, \tag{2.8}$$

which is the distance between the observer at time t and an object moving with the cosmological expansion at the speed of light. The Hubble horizon is a crucial quantity in the theory of structure formation and in the notion of quantum measurement in cosmology. It marks the boundary between the causal region centered at the observer O and the external region and roughly corresponds to the size of the observable universe (not to be confused with the physical dimensions of a closed universe parametrized by a). Actually, the true causal horizon is the *particle horizon*, defined as the sphere, centered at O, containing all the points which could have interacted with O through light signals since the "beginning" at $t = t_\mathrm{i}$ [24]. The radius of the sphere is

$$R_\mathrm{p} = a(t)\, r_\mathrm{p} := a(t) \int_{t_\mathrm{i}}^{t} \mathrm{d}t' \frac{c}{a(t')} = a(t) \int_{a_\mathrm{i}}^{a(t)} \mathrm{d}a \frac{c}{Ha^2}\,. \tag{2.9}$$

We will see that, in some cases, the particle and Hubble horizon are approximately the same. Also, when the comoving particle horizon is zero at t_i,

$$r_\mathrm{p} = c\tau\,. \tag{2.10}$$

We will almost always use natural units, so that from now on we trade the symbol $r_{\rm p}$ with τ. The context will make it clear whether τ is a distance (comoving particle horizon) or conformal time.[3]

The value of the Hubble parameter today is measured combining data on type Ia supernovæ, galaxy distributions and CMB observations:

$$\begin{aligned} H_0 &= 100\,h\,\mathrm{km\,s^{-1}\,Mpc^{-1}} \\ &\approx 3.336\,h\times 10^{-1}\,\mathrm{Gpc^{-1}} \\ &\approx 1.747\,h\times 10^{-61} m_{\rm Pl} \\ &\approx 2.133\,h\times 10^{-42}\mathrm{GeV}\,. \end{aligned} \tag{2.11}$$

The PLANCK 2015 value combining information on the temperature spectrum, on the polarization spectra at low multipoles and on lensing reconstruction ("PLANCK TT+lowP+lensing" likelihood) is [14]

$$h = 0.678 \pm 0.009 \quad (68\,\%\,\mathrm{CL})\,, \tag{2.12}$$

where the error is at the 68 % confidence level (CL) and includes statistical and systematic uncertainties.[4] Estimates change for different experiments and data sets in the same experiments, but they generally agree (see [12] for WMAP and [14] for other likelihood analyses within PLANCK).

Lower bounds on the age of the universe t_0 can be obtained from estimates of the age of astrophysical objects (e.g., globular clusters) or gamma-ray bursts, but a more precise value is found from the Hubble parameter:

$$t_0 \simeq H_0^{-1} = 9.786 h^{-1}\,\mathrm{Gyr}\,, \tag{2.13}$$

where Gyr is one billion years. With (2.12), one obtains $t_0 \sim 14.4\,\mathrm{Gyr}$. An $O(1)$ correction factor in the above formula, depending on the various energy components, can refine this estimate (see Problem 2.1). According to the PLANCK TT+lowP+lensing likelihood [14],

$$t_0 = 13.799 \pm 0.038\,\mathrm{Gyr} \quad (68\,\%\,\mathrm{CL})\,. \tag{2.14}$$

[3] Throughout this book, we shall call "universe" the spacetime region causally connected with the observer, while storing the name "Universe" with capital U for the whole spacetime, inclusive of the regions outside the horizon.

[4] Although errors are bound to change as soon as new measurements become available, we report them to give the reader an idea of the level of accuracy of modern observations. The student should take these numbers with a critical attitude. Where do they come from? How do they change if one varies the data samples and the prior constraints? Is a model still acceptable if it predicts numbers outside the 1σ experimental interval? (The answer to the last question is Yes. One should start worrying, or getting excited, only when the model offshoots beyond the 3σ level.)

2.2 Einstein and Continuity Equations

In this section, we introduce the classical total action and equations of motion of general relativity in D dimensions. Our conventions for the Levi-Civita connection, Riemann and Ricci tensors, and Ricci scalar are

$$\Gamma^{\rho}_{\mu\nu} := \tfrac{1}{2} g^{\rho\sigma} \left(\partial_\mu g_{\nu\sigma} + \partial_\nu g_{\mu\sigma} - \partial_\sigma g_{\mu\nu} \right) , \tag{2.15}$$

$$R^{\rho}_{\ \mu\sigma\nu} := \partial_\sigma \Gamma^{\rho}_{\mu\nu} - \partial_\nu \Gamma^{\rho}_{\mu\sigma} + \Gamma^{\tau}_{\mu\nu} \Gamma^{\rho}_{\sigma\tau} - \Gamma^{\tau}_{\mu\sigma} \Gamma^{\rho}_{\nu\tau} , \tag{2.16}$$

$$R_{\mu\nu} := R^{\rho}_{\ \mu\rho\nu} , \qquad R := R_{\mu\nu} g^{\mu\nu} . \tag{2.17}$$

The *Ansatz* of general relativity is the Einstein–Hilbert gravitational action

$$\boxed{S_g = \frac{1}{2\kappa^2} \int \mathrm{d}^D x \, \sqrt{-g} \, (R - 2\Lambda) \, ,} \tag{2.18}$$

where $g := \det(g_{\mu\nu})$ is the determinant of the dimensionless metric $g_{\mu\nu}$, $\kappa^2 = 8\pi G$ is D-dimensional Newton's constant, and Λ is the *cosmological constant*. The couplings have dimension

$$[\kappa^2] = 2 - D \, , \qquad [\Lambda] = 2 \, . \tag{2.19}$$

In a spacetime with $D = 2$ dimensions, the Newton constant is dimensionless, the Einstein–Hilbert action is a topological invariant and there are no dynamical gravitational degrees of freedom. The Newton constant has negative energy dimensionality for $D > 2$, a fact of utmost importance for the renormalization properties of a quantum theory of gravity (Sect. 8.2).

The gravitational action is second order in spacetime derivatives. It can be augmented by higher-order curvature terms (Sect. 7.5) but there is no immediate need to do so because standard general relativity already explains most of the large-scale observations.

The constant Λ in (2.18) was originally introduced by Einstein in order to have stationary-universe solutions. After the discovery of cosmic expansion by Hubble in 1929, stationary cosmology was abandoned in favour of the big bang model and Λ was dropped. In the last years, however, the cosmological constant has been regaining the interest of the community thanks also to the advancements in astronomical and cosmological observations.

Assuming that matter is *minimally coupled* with gravity, the total action is

$$S = S_g + S_\partial + S_{\mathrm{m}} \, , \tag{2.20}$$

where S_g is (2.18) and $S_{\mathrm{m}} = \int \mathrm{d}^D x \sqrt{-g} \mathcal{L}_{\mathrm{m}}$ is the matter action. The piece S_∂, which will be further discussed in Sect. 9.1.4, is the *York–Gibbons–Hawking boundary*

term (first written by Einstein [25]) added for consistency with the variational principle [26, 27]. In fact, the latter only requires that variations of the metric be zero at the boundary (i.e., the geometry of the boundary is fixed) but, in general, the normal first derivatives may be non-vanishing. In order to take this issue into account and obtain the Einstein equations correctly, one must add a specific S_∂ to the total action. Unless stated otherwise, throughout the book we will ignore the boundary term either because we consider closed manifolds (which have no boundary) or just for simplicity of presentation.

To find the equations of motion (Einstein equations) we need the variations (see Sect. 3.1.1)

$$\delta\sqrt{-g} = -\tfrac{1}{2}\, g_{\mu\nu}\, \sqrt{-g}\, \delta g^{\mu\nu}\,, \tag{2.21}$$

$$\delta R = (R_{\mu\nu} + g_{\mu\nu}\,\Box - \nabla_\mu \nabla_\nu)\, \delta g^{\mu\nu}\,, \tag{2.22}$$

where $\nabla_\nu V_\mu := \partial_\nu V_\mu - \Gamma^\sigma_{\mu\nu} V_\sigma$ is the covariant derivative of a vector V_μ and $\Box = \nabla_\mu \nabla^\mu$ is the curved d'Alembertian or Laplace–Beltrami operator. From (2.20), the Einstein equations $\delta S/\delta g^{\mu\nu} = 0$ read

$$\boxed{G_{\mu\nu} + g_{\mu\nu}\Lambda = \kappa^2 T_{\mu\nu}\,,} \tag{2.23}$$

where

$$G_{\mu\nu} := R_{\mu\nu} - \frac{1}{2} g_{\mu\nu} R\,, \tag{2.24}$$

$$T_{\mu\nu} := -\frac{2}{\sqrt{-g}} \frac{\delta S_{\rm m}}{\delta g^{\mu\nu}} = -2\frac{\partial \mathcal{L}_{\rm m}}{\partial g^{\mu\nu}} + g_{\mu\nu}\mathcal{L}_{\rm m}\,. \tag{2.25}$$

Taking the trace of (2.23) gives

$$-\left(\frac{D}{2} - 1\right) R + D\Lambda = \kappa^2 T^{\ \mu}_{\mu}\,. \tag{2.26}$$

$T_{\mu\nu}$ is the *energy-momentum tensor* (or stress-energy tensor) of matter. Its definition determines the continuity equation. In fact, let

$$\delta S_{\rm m} = \frac{1}{2} \int {\rm d}^D x\, \sqrt{-g}\, T^{\mu\sigma}\, \delta g_{\mu\sigma} \tag{2.27}$$

be the infinitesimal variation of the matter action with respect to the external field $\delta g_{\mu\sigma}$. For a constant infinitesimal coordinate transformation

$$x^{\mu\prime} = x^\mu + \delta x^\mu\,, \qquad \delta x^\nu = -a^\nu\,, \tag{2.28}$$

one has

$$\delta g_{\mu\sigma} = g_{\nu\sigma}\partial_\mu a^\nu + g_{\mu\nu}\partial_\sigma a^\nu + a^\nu \partial_\nu g_{\mu\sigma}\,, \tag{2.29}$$

where we used the definition of the Lie derivative for rank-2 and rank-0 tensors (see Chap. 3). Plugging (2.29) into (2.27) and integrating by parts, we get

$$\delta S_{\rm m} = -\int {\rm d}^D x\, a^\nu \left[\partial_\mu(\sqrt{-g}T^\mu_{\ \nu}) - \frac{1}{2}\sqrt{-g}T^{\mu\sigma}\partial_\nu g_{\mu\sigma}\right]. \tag{2.30}$$

Invariance of the action under diffeomorphisms requires $\delta S_{\rm m}$ to vanish *on shell* (i.e., when the dynamical equations are satisfied). Using the properties of the Levi-Civita connection (2.15) and the definition of the covariant derivative of a rank-2 tensor,

$$\begin{aligned}\nabla_\mu T^\mu_{\ \nu} &= \partial_\mu T^\mu_{\ \nu} + \Gamma^\mu_{\mu\sigma}T^\sigma_{\ \nu} - \Gamma^\sigma_{\mu\nu}T^\mu_{\ \sigma} \\ &= \frac{1}{\sqrt{-g}}\partial_\mu\left(\sqrt{-g}T^\mu_{\ \nu}\right) - \frac{1}{2}(\partial_\nu g_{\mu\sigma})T^{\mu\sigma}\,,\end{aligned}$$

one finally obtains the continuity equation

$$\boxed{\nabla_\mu T^\mu_{\ \nu} = 0\,.} \tag{2.31}$$

The energy-momentum tensor carries the contribution of all forms of energy in the universe, except gravity.

The continuity and Einstein equations are not independent because of the contracted Bianchi identities

$$2\nabla^\mu R_{\mu\nu} = \nabla_\nu R\,. \tag{2.32}$$

The divergence of (2.23) correctly reproduces (2.31).

2.2.1 Energy Conditions

The matter sector can be classified according to a set of covariant conditions [28]. Consider an arbitrary future-directed time-like vector t^μ ($t_\mu t^\mu < 0$; see Sect. 6.1.1) and a null vector n^μ ($n_\mu n^\mu = 0$). The *null energy condition* (NEC) is

$$T_{\mu\nu}n^\mu n^\nu \geqslant 0 \qquad \forall\, n^\mu \text{ null}\,. \tag{2.33}$$

When the Einstein equations (2.23) hold, this is equivalent to the *null convergence condition*

$$R_{\mu\nu}n^\mu n^\nu \geqslant 0 \qquad \forall\, n^\mu \quad \text{null}\,. \tag{2.34}$$

We will use this form of the NEC in Chap. 6.

The *weak energy condition* (WEC) states that

$$T_{\mu\nu}t^\mu t^\nu \geqslant 0 \qquad \forall\, t^\mu \text{ time-like}\,. \tag{2.35}$$

In particular, given the unit time-like vector u^μ ($u_\mu u^\mu = -1$), the matter energy density

$$\rho := T_{\mu\nu}u^\mu u^\nu \tag{2.36}$$

is always non-negative. Most of the known matter fields obey the NEC and WEC. Exceptions are condensates, which admit negative-energy states. Violations of the WEC can also come from quantum effects (Casimir energy, squeezed states, and so on).

The *dominant energy condition* (DEC) requires that $-T_{\mu\nu}t^\mu$ is either future-directed or null,

$$-T_{\mu\nu}t^\mu = Au^\mu + Bn^\mu\,, \tag{2.37}$$

where $A, B > 0$. In other words, momentum cannot (be observed to) flow faster than light (causal flux). In particular, the DEC implies the WEC.

The *time-like convergence condition* requires that

$$R_{\mu\nu}t^\mu t^\nu \geqslant 0 \qquad \forall\, t^\mu \text{ time-like}\,. \tag{2.38}$$

If the Einstein equations hold, this is equivalent to the *strong energy condition* (SEC)

$$\left(T_{\mu\nu} - \frac{1}{D-2}g_{\mu\nu}T_\sigma^{\ \sigma} + \frac{2}{D-2}g_{\mu\nu}\frac{\Lambda}{\kappa^2}\right)t^\mu t^\nu \geqslant 0\,. \tag{2.39}$$

2.3 Perfect Fluid

The energy-momentum tensor assumes a simple form when the only matter content of the universe is a *perfect fluid* (zero heat flow and anisotropic stress). Its definition is

$$\boxed{T_{\mu\nu} = (\rho + P)\,u_\mu u_\nu + P\,g_{\mu\nu}\,,} \tag{2.40}$$

where $\rho = T_{00}$ and $P = T_\alpha^{\ \alpha}/(D-1)$ are the energy density and pressure of the fluid, $u^\mu = \mathrm{d}x^\mu/\mathrm{d}t$ is the comoving D-velocity (unit time-like vector, $u_\mu u^\mu = -1$) tangent to a fluid element's world-line, and t is proper time along the fluid world-line. Since we are in a globally hyperbolic spacetime, u^μ also corresponds to the unit vector normal to spatial Cauchy surfaces. The metric $g_{\mu\nu}$ induces a Riemannian metric $h_{\mu\nu}$ defined by the *first fundamental form*

$$h_{\mu\nu} = g_{\mu\nu} + u_\mu u_\nu\,, \qquad h_\mu^{\ \nu} = h_\mu^{\ \sigma} h_\sigma^{\ \nu}\,, \qquad u^\mu h_\mu^{\ \nu} = 0\,, \tag{2.41}$$

which is the metric spatial projection orthogonal to the comoving velocity.

At every point of spacetime, the local rest frame of a fluid is defined as the coordinate system where the off-diagonal components of the fluid vanish, $T^{0\alpha} = 0$, and

$$u^\mu = \delta_0^\mu = ((-g_{00})^{-1/2}, 0, \ldots, 0)^\mu\,. \tag{2.42}$$

In covariant formalism [29–31], the gradient of the four-velocity field is decomposed as

$$\nabla_\nu u_\mu = \sigma_{\mu\nu} + \omega_{\mu\nu} + \frac{1}{D-1}\theta h_{\mu\nu} - \dot{u}_\mu u_\nu\,. \tag{2.43}$$

Here,

$$\sigma_{\mu\nu} := \nabla_{(\nu} u_{\mu)} - \frac{1}{D-1}\theta h_{\mu\nu} + \dot{u}_{(\mu} u_{\nu)} = h_{\sigma(\nu}\nabla^\sigma u_{\mu)} - \frac{1}{D-1}\theta h_{\mu\nu} \tag{2.44}$$

is the symmetric *shear* tensor,

$$\omega_{\mu\nu} := \nabla_{[\nu} u_{\mu]} + \dot{u}_{[\mu} u_{\nu]} = h_{\sigma[\nu}\nabla^\sigma u_{\mu]} \tag{2.45}$$

is the anti-symmetric *vorticity* tensor,

$$\theta := \nabla^\mu u_\mu \tag{2.46}$$

is the *volume expansion* (or expansion of the family of time-like geodesics u_μ) and a dot defines the proper-time derivative

$$\dot{} := u_\mu \nabla^\mu\,. \tag{2.47}$$

Integrating the volume expansion along a world-line with respect to t, one defines the *number of e-foldings*

$$\mathcal{N}_a := \frac{1}{D-1}\int_{t_\mathrm{i}}^{t} \mathrm{d}t'\,\theta\,, \tag{2.48}$$

where $t_{\rm i}$ is some initial time. This definition is unique up to an integration constant for each world-line, which can be fixed by choosing a reference hypersurface where $\mathcal{N}_a = 0$.

The continuity equation (2.31) contracted with $-u^\nu$ is

$$\dot{\rho} + (\theta - \sigma)(\rho + p) = 0\,, \tag{2.49}$$

where $\sigma = \sigma_\mu{}^\mu = u^\mu \dot{u}_\mu$. This equation is exact and valid at all scales. Contracting (2.31) with $h_\rho{}^\nu$, we get

$$D_\mu p + h_\mu{}^\nu \dot{u}_\nu (\rho + p) = 0\,, \tag{2.50}$$

where

$$D_\mu := h_\mu{}^\nu \nabla_\nu = \nabla_\mu + u_\mu u^\nu \nabla_\nu \tag{2.51}$$

is the spatial projection of the covariant derivative. Equation (2.50) can also be written as

$$u_\mu \dot{P} + (\dot{u}_\mu + \sigma u_\mu)(\rho + P) + \nabla_\mu P = 0\,. \tag{2.52}$$

Defining the effective *barotropic index*

$$w := \frac{P}{\rho}\,, \tag{2.53}$$

the energy conditions of the previous section are readily translated into conditions on (2.53). The NEC is

$$\text{NEC:} \qquad \rho(1 + w) \geqslant 0\,, \tag{2.54}$$

and is implied by all the other conditions. In fact, one can write any time-like vector of modulus $|t|$ as $t^\mu = |t| u^\mu + n^\mu$. Contracting t^μ with (2.40) according to the given condition (2.35), (2.37) or (2.39), and then sending $|t|$ to zero, one always reobtains (2.54). The WEC, DEC and SEC then are

$$\text{WEC:} \qquad \rho \geqslant 0\,, \qquad w \geqslant -1\,, \tag{2.55}$$

$$\text{DEC:} \qquad \rho \geqslant |P|\,, \qquad -1 \leqslant w \leqslant 1\,, \tag{2.56}$$

$$\text{SEC:} \qquad \rho[(D-3) + (D-1)w] - \frac{2\Lambda}{\kappa^2} \geqslant 0\,, \tag{2.57}$$

while

$$\text{DEC} + \text{SEC}(\Lambda = 0): \qquad -\frac{D-3}{D-1} \leqslant w \leqslant 1\,. \tag{2.58}$$

In $D = 4$, (2.58) reads $-1/3 \leqslant w \leqslant 1$.

Summarizing,

$$\boxed{\text{DEC} \implies \text{WEC} \implies \text{NEC} \impliedby \text{SEC}(\Lambda = 0)\,.}$$

2.3.1 Scalar Field

If matter is a scalar field with potential $V(\phi)$, its Lagrangian density is

$$\mathcal{L}_{\rm m} = \mathcal{L}_\phi = -\frac{1}{2}\partial_\mu\phi\partial^\mu\phi - V(\phi)\,. \tag{2.59}$$

Scaling dimension (or engineering, or canonical dimension; in momentum units) of ϕ is

$$[\phi] = \frac{D-2}{2}\,, \tag{2.60}$$

while for a polynomial potential

$$V(\phi) = \sum_{n=0}^{N}\sigma_n\phi^n\,, \tag{2.61}$$

the engineering dimension of the couplings is

$$[\sigma_n] = D - \frac{n(D-2)}{2}\,. \tag{2.62}$$

It is straightforward to see that the scalar equation of motion $\delta S_{\rm m}/\delta\phi = 0$ is in agreement with (2.31). Invariance of the total action under the infinitesimal shift

$$\phi \to \phi + \delta\phi \tag{2.63}$$

yields the equation of motion

$$0 = \frac{\partial\mathcal{L}_\phi}{\partial\phi} - \frac{\mathrm{d}}{\mathrm{d}x^\mu}\frac{\partial\mathcal{L}_\phi}{\partial(\partial_\mu\phi)}\,. \tag{2.64}$$

From (2.59), we get

$$T^\mu_{\ \nu} = \delta^\mu_\nu\mathcal{L}_\phi + \partial^\mu\phi\partial_\nu\phi \tag{2.65}$$

and

$$\boxed{\Box\phi - V_{,\phi} = 0\,,} \tag{2.66}$$

where $V_{,\phi} = \partial V/\partial\phi$ and

$$\Box\phi = \frac{1}{\sqrt{-g}}\partial_\mu(\sqrt{-g}\partial^\mu\phi)\,. \tag{2.67}$$

The scalar field is a particular case of perfect fluid, with world-lines orthogonal to $\phi = \text{const}$ hypersurfaces [32]:

$$u_\mu = -\frac{\partial_\mu\phi}{\dot\phi}\,. \tag{2.68}$$

When $V \propto \phi^2$, (2.66) is called Klein–Gordon equation.

2.4 Friedmann Equations

On an FLRW background, the only non-vanishing Levi-Civita and Ricci components are

$$\Gamma^0_{\alpha\beta} = Hg_{\alpha\beta}, \qquad \Gamma^\beta_{\alpha 0} = H\delta^\beta_\alpha, \qquad \Gamma^\lambda_{\alpha\beta} = \Gamma^\lambda_{\alpha\beta}(\gamma_{\alpha\beta})\,, \tag{2.69}$$

and

$$R_{00} = -(D-1)(H^2+\dot H) = -(D-1)\frac{\ddot a}{a}\,, \tag{2.70}$$

$$R_{\alpha\beta} = \left[\frac{2\mathrm{K}}{a^2} + (D-1)H^2 + \dot H\right] g_{\alpha\beta}\,, \tag{2.71}$$

$$\begin{aligned} R &= {}^{(D-1)}R + (D-1)\left(DH^2 + 2\dot H\right) \\ &= (D-1)\left(\frac{2\mathrm{K}}{a^2} + DH^2 + 2\dot H\right), \end{aligned} \tag{2.72}$$

where we have exploited the symmetries of the space-like hypersurface $\tilde\Sigma$ [33] and ${}^{(D-1)}R$ is its Ricci scalar.

For simplicity we assume that the universe is filled by a perfect fluid, (2.40). The FLRW shear and viscosity vanish, while the volume expansion and the Hubble

parameter coincide,

$$\theta = (D-1)H\,, \qquad \mathcal{N}_a = \ln\frac{a}{a_{\rm i}}\,. \tag{2.73}$$

The 00 component of the Einstein equations (2.23) is

$$\left(\frac{D}{2}-1\right)H^2 = \frac{\kappa^2}{D-1}\rho + \frac{\Lambda}{D-1} - \frac{\mathrm{K}}{a^2}\,, \tag{2.74}$$

while combining that with the trace equation (2.26) one obtains

$$-(D-2)\left(H^2+\dot{H}\right) + \frac{2\Lambda}{D-1} = \frac{\kappa^2}{D-1}\left[(D-3)\rho + (D-1)P\right]. \tag{2.75}$$

The continuity equation (2.49) has no shear and becomes

$$\dot{\rho} + (D-1)H(\rho+P) = 0\,, \tag{2.76}$$

while (2.52) is trivial in the fluid rest frame. For a barotropic fluid $p = w\rho$, w is constant and the continuity equation is solved by

$$\rho = \rho_0\, a^{-(D-1)(1+w)}, \tag{2.77}$$

where $a_0 = a(t_0) = 1$. From (2.74) with $\Lambda = 0 = \mathrm{K}$, it follows that

$$a = \left(\frac{t}{t_0}\right)^{\frac{2}{(D-1)(1+w)}}\,. \tag{2.78}$$

For a scalar field,

$$\rho_\phi = \frac{\dot{\phi}^2}{2} + V\,, \qquad P_\phi = \mathcal{L}_\phi = \frac{\dot{\phi}^2}{2} - V\,, \tag{2.79}$$

and (2.76) becomes (2.66),

$$\ddot{\phi} + (D-1)H\dot{\phi} + V_{,\phi} = 0\,. \tag{2.80}$$

From now on we specialize to four dimensions, $D = 4$. In this case, we obtain the first and second *Friedmann equations*

$$\boxed{H^2 = \frac{\kappa^2}{3}\rho + \frac{\Lambda}{3} - \frac{\mathrm{K}}{a^2}\,,} \tag{2.81}$$

$$\boxed{\frac{\ddot{a}}{a} = H^2 + \dot{H} = -\frac{\kappa^2}{6}(\rho + 3P) + \frac{\Lambda}{3}\,.} \tag{2.82}$$

Equation (2.82) is the FLRW version of the Raychaudhuri equation (Problem 6.1).

2.5 Content of the Universe

Equation (2.82) can be rewritten in terms of the parameter Ω, defined as the ratio between the total energy density ρ and the critical density $\rho_{\rm crit}$ sufficient to stop the expansion:

$$\Omega := \frac{\rho}{\rho_{\rm crit}}\,, \qquad \rho_{\rm crit} := \frac{3H^2}{\kappa^2}\,. \tag{2.83}$$

Equation (2.81) with $\Lambda = 0$ becomes

$$\Omega - 1 = \Omega_{\rm K}\,, \tag{2.84}$$

where

$$\Omega_{\rm K} := \frac{\rm K}{a^2H^2} \tag{2.85}$$

is the deviation from the critical density. If the universe is spatially flat, $\Omega = 1$.

Let us now take point **(III)** of the recipe of the universe into account (Sect. 2.1.1). Apart from the intrinsic curvature term, the contributions to the total energy density ρ is typically divided into radiation ($\Omega_{\rm r}$, which includes photons), baryonic matter and non-baryonic matter ($\Omega_{\rm m} = \Omega_{\rm b} + \Omega_{\rm nb} + \Omega_\nu$, where we include also massive neutrinos).[5] In the view of explaining point **(IV)**, we also add an extra component we call Ω_Λ (which might or might not correspond to a non-vanishing Λ in (2.81)):

$$\Omega = \Omega_{\rm r} + \Omega_{\rm m} + \Omega_\Lambda + \Omega_{\rm K}\,. \tag{2.86}$$

2.5.1 Dust and Radiation

Regarded as a perfect fluid, each contribution obeys an independent continuity equation (2.76). The case $w = 1/3$ is radiation which redshifts away

[5] In general relativity and quantum gravity, one calls "matter" everything which is not geometry. We did so in Sect. 2.2 but here we use cosmology jargon and separate radiation from the rest of the "matter."

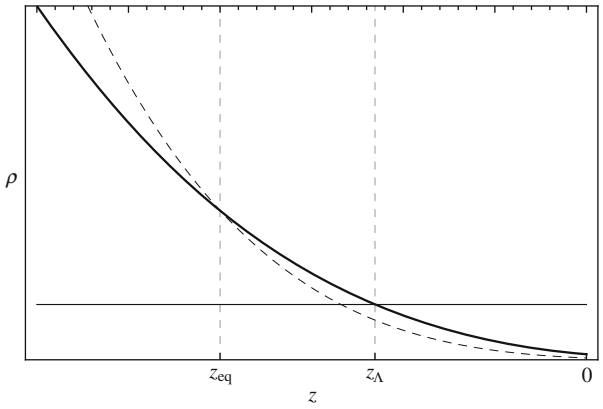

Fig. 2.8 Matter (*thick curve*), radiation (*dashed curve*), and cosmological constant (*thin line*) energy densities as functions of redshift. Radiation-matter and matter-dark energy equality times are indicated. The redshift scale is arbitrary

as (see (2.77))

$$\rho_{\rm r} = \rho_{\rm r0}(1+z)^4\,, \tag{2.87}$$

while $w = 0$ is pressureless (dust) matter,

$$\rho_{\rm m} = \rho_{\rm m0}(1+z)^3\,. \tag{2.88}$$

The radiation density decreases faster than matter density during the expansion ($z \to 0$). Therefore, the radiation component dominates over matter at early times, but matter eventually takes over (Fig. 2.8).

The moment[6] $t_{\rm eq}$ when the two densities coincide is called *equality*. When the universe is filled only with radiation and dust, the total energy density evolves as (2.87) when $z \geqslant z_{\rm eq}$, and as (2.88) otherwise. The redshift at equality is constrained by CMB observations (from the ratio of the first peak to the third peak of the power spectrum) combined with other observations. For the PLANCK TT+lowP+lensing likelihood [14],

$$z_{\rm eq} = 3365 \pm 44 \quad (68\,\%\,{\rm CL}). \tag{2.89}$$

Different data sets all converge to the rounded value

$$z_{\rm eq} \approx 3400\,, \tag{2.90}$$

[6] In an approximate sense: the transition is smooth, not point-wise.

which we will use in Sect. 2.7. Once the redshift of an object is found, one can calculate the corresponding age. In particular, radiation-matter equality happened when the universe was less than 10,000 years old (see Problem 2.2).

From (2.78), one can see that

$$a \sim t^{\frac{2}{3}}\,, \qquad w = 0\,, \tag{2.91}$$

$$a \sim t^{\frac{1}{2}}\,, \qquad w = \frac{1}{3}\,. \tag{2.92}$$

In these scenarios where the universe expands as a *power law* (p is a constant, not to be confused with pressure),

$$\boxed{a \sim t^p\,, \qquad p = \frac{2}{3(1+w)}\,, \qquad H = \frac{p}{t}\,,} \tag{2.93}$$

and when

$$w > -\frac{1}{3} \qquad (0 < p < 1) \tag{2.94}$$

holds, the particle horizon (2.9) is about the same as the Hubble horizon (2.8):

$$\begin{aligned} R_\mathrm{p} &= t^p \int_{t_\mathrm{i}}^{t} \mathrm{d}t' t'^{-p} \overset{t \gg t_\mathrm{i}}{\simeq} \frac{1}{1-p} t = \frac{p}{1-p} R_H \\ &\simeq R_H\,. \end{aligned} \tag{2.95}$$

Several properties of the particle and Hubble horizons and the size at different epochs can be found in Problems 2.3–2.6 (see also Sect. 3.1.3). Exact power-law solutions are the subject of Problem 2.11.

Recent estimates of radiation and matter density today are (for the PLANCK TT+lowP+lensing likelihood at 68 % CL) [14]

$$\Omega_{\mathrm{r}0} h^2 = 2.469 \times 10^{-5}\,, \tag{2.96}$$

$$\Omega_{\mathrm{b}0} h^2 = 0.02226 \pm 0.00023\,, \tag{2.97}$$

$$\Omega_{\mathrm{c}0} h^2 = 0.1186 \pm 0.0020\,, \tag{2.98}$$

$$\Omega_{\mathrm{m}0} h^2 = 0.1415 \pm 0.0019\,. \tag{2.99}$$

The difference between the total contribution of matter (measured from the dynamics of galaxy clusters) and baryonic matter (from the visible galaxy distribution) is ascribed to the presence of another non-baryonic component, dark matter (see [34] for a review). Dark matter does not interact with photons and it can be observed only indirectly. In (2.98), we indicated it as $\Omega_\mathrm{c} = \Omega_\mathrm{nb} + \Omega_\nu$. Ω_m is a derived

quantity obtained from the sum of baryonic and dark matter densities. Evidence is in favour of dark matter being made of particles moving at non-relativistic speed and lying outside the Standard Model of particle physics. Because of the weak or absent interaction with radiation, density fluctuations of non-baryonic dark matter can start growing much earlier than for ordinary matter, thus having time to tune their amplitudes at the level observed today in large-scale structures. Among the particle candidates from minimal extensions (supersymmetric and not) of the Standard Model are axions, sterile neutrinos and WIMPs (weakly interactive massive particles) such as neutralinos; experiments can place bounds on the abundances of these particles [35, 36]. There is also a possibility that gravity itself, via some modified action, may account for dark-matter effects. A small part of $\Omega_{\rm c}$ can be due to massive neutrinos, $\Omega_{\nu 0}h^2 < 0.0025$ (95 % CL) [14].

2.5.2 Hot Big Bang and the Big-Bang Problem

The quasi isotropy of the CMB temperature indicates that the early universe was in thermal equilibrium. Therefore, we can express the energy density of radiation and matter in terms of thermodynamical quantities such as the temperature T.

The most important processes through which radiation interacts with matter are three: single and double Compton scattering and Bremsstrahlung. *Single Compton scattering* describes the collision of a photon with a free electron,

$$\gamma(\nu) + e^- \longrightarrow \gamma(\nu') + e^- .$$

When the photon energy is small with respect to the rest mass of the electron, the scattering process can be approximated by *Thomson scattering*.

When an electron at rest collides with a photon, a negative energy transfer occurs from the electron to the photon, whose frequency ν red-shifts ($\nu' < \nu$). The combination of this effect with the inverse scattering, where a photon gains energy from a relativistic electron ($\nu' > \nu$), leads to thermal equilibrium. These are elastic processes and the number of photons is conserved. In the *double* or *inelastic Compton scattering*, on the other hand, photons are emitted or absorbed,

$$\gamma + e^- \longleftrightarrow \gamma + \gamma + e^- .$$

In the Coulomb interaction between an electron and an atomic nucleus X, the former is accelerated in the rest frame of the ion X and emits radiation. In this case, one has *thermal Bremsstrahlung*,

$$e^- + X \longleftrightarrow e^- + X + \gamma .$$

The inverse reaction may also happen, since charged particles can absorb photons.

The energy (temperature) of these processes determines which is the dominant effect:

- Bremsstrahlung for $1\,\mathrm{eV} < T < 90\,\mathrm{eV}$.
- Single Compton scattering for $90\,\mathrm{eV} < T < 1\,\mathrm{keV}$.
- Double Compton scattering for $T \gtrsim 1\,\mathrm{keV}$,

where $T = k_{\mathrm{B}} T_{\mathrm{K}}$ is measured in eV. All these processes have a characteristic velocity greater than the cosmic expansion and hence they modify the photon distribution of the cosmological plasma.

At equilibrium, the photons involved in Compton scattering obey a Bose–Einstein distribution

$$f(\omega) = \frac{1}{\mathrm{e}^{\frac{\hbar\omega}{T} - \mu} - 1}\,, \tag{2.100}$$

where $\omega = 2\pi\nu$ is the angular frequency and μ is the chemical potential, non-vanishing if the total number of photons is conserved. However, the number of low-frequency photons change due to inelastic Compton scattering and Bremsstrahlung, thus sending effectively μ to zero. In the meanwhile, elastic Compton scattering redistributes the photons over the spectrum. One then obtains a *black-body spectrum* of intensity (in $\hbar = 1$ units)

$$I(\omega, T) = \frac{\omega^3}{2\pi^2} f(\omega) = \frac{1}{2\pi^2} \frac{\omega^3}{\mathrm{e}^{\frac{\omega}{T}} - 1}\,. \tag{2.101}$$

Once equilibrium and the black-body spectrum are achieved, they are *preserved* both by the above processes and by cosmic expansion, whose effect is to rescale the spectrum while maintaining its form. We have seen in (2.6) that $\lambda \sim a$, so that $\omega \sim 1 + z$ and the ratio ω/T in (2.101) is unchanged if $T \sim 1 + z$. We can find the proportionality constant as follows. The distribution (2.100) defines the number density of bosons of the i-th species per unit volume, $\mathrm{d}n_i(\omega) = \mathrm{d}^3\omega\, g_i (2\pi)^{-3} f(\omega)$, where g_i is the number of spin states ($g_\gamma = 2$ for photons). Therefore, the energy density of a species with black-body distribution is the integral of $\mathrm{d}n(\omega)\,\omega$ over all frequencies ($\mathrm{d}^3\omega = 4\pi\,\mathrm{d}\omega\,\omega^2$), which is the integrated intensity

$$\begin{aligned} \rho_i &= \int_0^{+\infty} \mathrm{d}n_i(\omega)\,\omega = g_i \int_0^{+\infty} \mathrm{d}\omega\, I(\omega, T) \\ &\overset{x=\omega/T}{=} \frac{g_i(T)}{2\pi^2} T^4 \int_0^{+\infty} \mathrm{d}x \frac{x^3}{\mathrm{e}^x - 1} = \frac{\pi^2}{30} g_i T^4\,. \end{aligned}$$

One should sum over all species i in thermal equilibrium ($\mu_i \ll T$), including fermions. The latter obey a Fermi–Dirac distribution $f(\omega) = (\mathrm{e}^{\omega/T - \mu} + 1)^{-1}$, resulting in a contribution $(7/8) g_i$ for each species. The total energy density of

radiation is the Stefan–Boltzmann law with g_i replaced by a total effective $g_*(T)$:

$$\rho_{\rm r} = \frac{\pi^2}{30} g_*(T)\, T^4 \,. \tag{2.102}$$

The coefficient $g_*(T) = O(1) - O(10)$ is temperature dependent because a species with mass m_i no longer participates in (2.102) when the temperature falls below m_i. Away from these *decoupling* events, g_* can be regarded as constant. For a radiation-dominated universe, comparing (2.102) with (2.87) one gets the temperature as a function of redshift:

$$\begin{aligned} T &= \left(\frac{30}{\pi^2}\frac{\rho_{\rm r0}}{g_*}\right)^{1/4}(1+z) \simeq 3.96\left(\frac{\Omega_{\rm r0}h^2}{g_*}\right)^{1/4}(1+z)\times 10^{-3}\,{\rm eV} \\ &\overset{(2.96)}{\approx} \frac{2.79}{g_*^{1/4}}(1+z)\times 10^{-4}\,{\rm eV} \qquad (2.103) \\ &\approx \frac{3.24}{g_*^{1/4}}(1+z)\,{\rm K}\,. \qquad (2.104) \end{aligned}$$

Using (2.81) and (2.92), one has

$$H = \frac{m_{\rm Pl}t_{\rm Pl}}{2t}\,, \tag{2.105}$$

so that, with (2.81),

$$t = \left(\frac{45}{16\pi^3 g_*}\right)^{1/2}\frac{m_{\rm Pl}^2 t_{\rm Pl}}{T^2} \approx \frac{2.42}{g_*^{1/2}}\left(\frac{10^6{\rm eV}}{T}\right)^2 {\rm s}\,. \tag{2.106}$$

With these formulæ, one can calculate the temperature at a given redshift and the age of the universe at a given temperature (see Problem 2.8).

Since $T \propto 1+z$, one concludes that the universe was a high-temperature, radiation-dominated plasma in early epochs. This is why the standard model is called *hot*. As in the great majority of cosmological solutions, the power-law profile (2.93) tends to $a \to 0$ in the past. At the *big bang* $t = 0$ (the earliest instant ever), the metric is singular and general relativity breaks down. The Universe reduces to a point of infinite temperature and energy density. Generic classical cosmological solutions do possess a big-bang singularity and one cannot trust the theory at the very beginning. This is clearly a problem of self-consistency which is desirable to solve. We will talk about it much later (Chaps. 6, 10 and 13).

2.5.3 Dark Energy and the cosmological Constant Problem

The hot big bang model works very well from early ages until almost today. This is the main reason why we assumed that only dust and radiation are present. Other types of fluid, if added, should first prove themselves necessary to explain experimental data, and then find their place in a field-theory model. For example, an extra *stiff matter* component ($w = 1$) would scale as $\rho_{\rm stiff} = \rho_{\rm stiff0}(1+z)^6$ and it would dominate at early times. Let $\tilde{z}_{\rm eq}$ be the redshift when $\rho_{\rm stiff} = \rho_{\rm r}$. The hot big bang model is verified to a high degree of accuracy starting from the *big-bang nucleosynthesis* (BBN; see Problem 2.8) at $z_{\rm BBN} \sim 10^9$, so that $\tilde{z}_{\rm eq} > z_{\rm BBN}$. From (2.96), one must have $\Omega_{\rm stiff0}h^2 \lesssim 10^{-23}$, and any such component would be unobservable today. Therefore, there is no need to consider stiff matter.

On the other hand, from the positivity of ρ, (2.82) and the strong energy condition (2.57) with $\Lambda = 0$, it follows that a universe filled only with matter and radiation must decelerate, $\ddot{a} < 0$. This is in contrast with point **(IV)** so that, after all, we do have to add some other contribution to the total energy density. So far, we have ignored the cosmological constant. Let us rewrite the Friedmann equations (2.81)–(2.82):

$$\frac{\ddot{a}}{a} = -\frac{\kappa^2}{6}[(\rho + \rho_\Lambda) + 3(P + P_\Lambda)]\,, \tag{2.107}$$

$$H^2 = \frac{\kappa^2}{3}(\rho + \rho_\Lambda) - \frac{\mathrm{K}}{a^2}\,, \tag{2.108}$$

where

$$\rho_\Lambda = -P_\Lambda := \frac{\Lambda}{\kappa^2}\,. \tag{2.109}$$

A particular solution of these Friedmann equations is the *de Sitter universe* [37], a cosmological model without matter ($\rho = 0$) and flat spatial sections ($\mathrm{K} = 0$):

$$\boxed{H = \sqrt{\frac{\Lambda}{3}} \qquad \Rightarrow \qquad a(t) = a(0)\,\mathrm{e}^{Ht}\,.} \tag{2.110}$$

The Hubble rate is *constant* and the scale factor expands exponentially. It is the prototypical inflationary background and the cosmology with the simplest analytic properties (see Problem 2.10). It has an analogue also for a closed universe ($\mathrm{K} = 1$):

$$a(t) = H^{-1}\cosh(Ht)\,, \tag{2.111}$$

where $H = \sqrt{\Lambda/3}$.

In a quantum field theory context, ρ_Λ and p_Λ represent the energy density and pressure of quantum fluctuations of the vacuum. At the semi-classical level, gravity can be treated as classical, while Einstein equations take the form [38]

$$G_{\mu\nu} = \kappa^2 \langle T_{\mu\nu} \rangle \,, \tag{2.112}$$

which can be argued to be valid when dispersion in the phase of matter wave-functions is negligible [39]. In a local inertial frame, Lorentz invariance requires that the vacuum expectation value of the energy-momentum tensor be proportional to the Minkowski metric, $\langle T_{\mu\nu} \rangle \propto \eta_{\mu\nu}$. Therefore, in a general frame [40, 41]

$$\langle T_{\mu\nu} \rangle = -\rho_{\rm vac}\, g_{\mu\nu} \,. \tag{2.113}$$

This is a cosmological-constant contribution $\rho_{\rm vac} = \Lambda/\kappa^2 = \rho_\Lambda$ and the "vacuum equation of state" is (2.109), corresponding to the barotropic index

$$w_\Lambda = -1 \,. \tag{2.114}$$

The fact that the pressure P_Λ is negative should not worry the reader. In fact, in gravity the quantity P loses its usual meaning of thermodynamical pressure; here, it encodes a generic effect of "anti-gravitational repulsion."

A notable feature of the de Sitter universe is that it accelerates,

$$\frac{\ddot{a}}{a} = H^2 \Omega_\Lambda > 0 \,. \tag{2.115}$$

Measuring the redshift of type I supernovæ, in 1997 it was discovered that the universe is indeed accelerating [18, 42, 43]. First estimates gave $0.3 \leqslant \Omega_{\Lambda 0} \leqslant 0.9$. The advance in what is now called precision cosmology can be appreciated by comparing this early constraint with the most recent one to date from CMB observations [14] (PLANCK TT+lowP+lensing),

$$\Omega_{\Lambda 0} = \frac{\Lambda}{3H_0^2} = 0.692 \pm 0.012 \quad (68\,\%\ \text{CL}) \,, \tag{2.116}$$

or from the combination of data [14] about the CMB, supernovæ [6], baryon acoustic oscillations (BAO) [5, 44–48] and H_0 ("PLANCK TT+lowP+lensing+ext" likelihood):

$$\Omega_{\Lambda 0} = 0.6935 \pm 0.0072 \quad (68\,\%\ \text{CL}) \,. \tag{2.117}$$

Using (2.116),

$$\rho_\Lambda = \Omega_{\Lambda 0} \frac{3H_0^2}{\kappa^2} \approx 5.4 \times 10^{-123} m_{\rm Pl}^4 \approx (3.3 \times 10^{-3}\text{eV})^4 \,. \tag{2.118}$$

This is a very low density, about $10^{-29}\,\mathrm{g\,cm^{-3}}$, which would be extremely difficult to detect in the laboratory. Nevertheless, it constitutes about 70 % of the total density, since it uniformly fills the universe and all the regions otherwise empty of matter.

The experimental value w_0 of w_Λ today varies according to the prior constraints (zero or non-zero curvature, constant or varying w_Λ, and so on). For instance, for a constant w_Λ and a flat universe [14] (PLANCK TT+lowP+lensing+ext),

$$w_0 = -1.006^{+0.085}_{-0.091} \quad (95\,\%\ \mathrm{CL})\,. \tag{2.119}$$

Somewhat weaker bounds come from redshift-space distortions [49–51]. Letting $a(t_0) = a_0 = 1$ be the present value of the scale factor, a two-parameter model of a varying w_Λ is [52, 53]

$$w_\Lambda =: w_0 + w_a(a-1)\,, \tag{2.120}$$

so that today $w = w_0$. In this case, the PLANCK TT+lowP+lensing+ext posteriors are

$$-1.2 < w_0 < -0.6\,, \qquad -1.5 < w_a < 0.6 \qquad (95\,\%\ \mathrm{CL})\,. \tag{2.121}$$

A cosmological constant is the simplest explanation of late-time acceleration. However, Λ is a problematic object in many respects. Other "small" numbers do appear in cosmology but, usually, they are described by known physics and are not perceived as troublesome as (2.118) [54]. An instance is the energy density of matter or radiation at the time of equality,

$$\rho_{\mathrm{eq}} \approx 2.4 \times 10^{-113} m_{\mathrm{Pl}}^4\,, \tag{2.122}$$

which depends on the number density of photons and matter particles and can be calculated within the framework of standard high-energy physics [55]. On the other hand, the cosmological constant problem consists in the "unnatural" smallness of the quantity (2.118). There is an issue of fine tuning both at the classical level (via the ratio $\rho_\Lambda/\rho_{\mathrm{eq}} \approx 10^{-10}$) and in an effective quantum field theory set-up. Consider microscopic quantum degrees of freedom described by states with proper momentum $p < p_{\mathrm{max}}$, and assume a uniform distribution of the number of states per unit volume in momentum space, $\mathrm{d}^3\mathbf{p}\, n(p) \sim \mathrm{d}^3\mathbf{p}$. Then, the vacuum energy density due to these quantum states is (see Sect. 7.1)

$$\rho_{\mathrm{vac}} \sim \rho_{\mathrm{vac},0} \sim \int_0^{p_{\mathrm{max}}} \mathrm{d}p\, p^3 \sim p_{\mathrm{max}}^4\,, \tag{2.123}$$

where $p = |\mathbf{p}|$ and p_{max} is a cut-off above which the effective theory breaks down. We would expect that

$$p_{\mathrm{max}} \sim m_{\mathrm{Pl}} \sim 10^{19}\,\mathrm{GeV} \tag{2.124}$$

at the Planck scale, or that

$$p_{\max} = M_{\rm SUSY} > 10^{-16}\, m_{\rm Pl} \sim 10^3\,{\rm GeV} \tag{2.125}$$

for supersymmetry. If, as suggested above, Λ is the energy contribution of vacuum, then observations impose that $\rho_{\rm vac}^{1/4} = \rho_\Lambda^{1/4} \sim 10^{-31} m_{\rm Pl} \sim 10^{-3}\,{\rm eV}$, much smaller than (2.124) or (2.125). Therefore, there must be a contribution V_0 to the potential of the effective theory cancelling vacuum effects almost exactly. A calculation in the Standard Model of particles predicts too small a V_0, insufficient to meet the experimental value (2.118). On the other hand, supersymmetry overshoots the target and vacuum effects are cancelled exactly ($\Lambda = 0$); however, supersymmetry is broken at low energy scales, thus reducing but not removing the fine tuning. This is one formulation of the cosmological constant problem, which we will study in greater detail in Chap. 7.

Also, the universe has been accelerating only since $\ddot{a} = 0$, at (varying-w_Λ parametrization [56])

$$z_{\rm acc} = 0.81 \pm 0.30 \quad (95\,\%\ {\rm CL})\,, \tag{2.126}$$

that is, 6.8 ± 1.4 billion years ago. For a constant $\Lambda = \Lambda_0$, that epoch would be marked as somewhat special in the history of the universe, because it would be triggered by a non-thermodynamical effect. In other words, the model would depend on the initial condition $\Lambda = \Lambda_0$ (*coincidence problem*).

Notice that $z_{\rm acc}$ is larger than the redshift z_Λ at which $\rho_{\rm m} = \rho_\Lambda$: the onset of acceleration is before the cosmological constant dominates over matter (see [56] for a discussion). Figure 2.8 shows the evolution of the matter, radiation, and Λ energy densities.

There may be other candidates, cloaked under the mysterious name of *dark energy*, driving acceleration and accounting for the contribution (2.116) (see Problem 2.9). In the vacuum interpretation, the cosmological "constant" naturally varies with time, since the vacuum energy is temperature dependent. A running $\Lambda(t)$ better accommodates the coincidence problem and can be realized by a number of mechanisms. One of the most popular is *quintessence*, a dynamical scalar field operating like the inflaton but at different energy scales. The equation of state of a single homogeneous scalar spans the whole range of the DEC and, in general, models dominated by an energy component with $w < -1/3$ always accelerate:

$$\frac{\ddot{a}}{a} = -\frac{1}{2} H^2 (1 + 3w) \Omega\,. \tag{2.127}$$

However, due to the observational constraint $w \approx -1$ the quintessence field must be very similar to a cosmological constant and its dynamics is subject to a certain amount of fine tuning.

2.5.4 Spatial Curvature and Topology

The curvature contribution $\Omega_{\rm K}$ can be constrained by combining CMB data (mainly the position of the temperature power spectrum peaks, plus polarization) with distance indicators. In the so-called ΛCDM *concordance model* (Cold Dark Matter with a pure cosmological constant, $w_\Lambda = -1$), one has (PLANCK TT+lowP+lensing+BAO [14])

$$\Omega_{\rm K0} = 0.000 \pm 0.005 \quad (95\,\%\ \text{CL})\,. \tag{2.128}$$

The constraint changes according to data pools, but it is always compatible with flat geometry.

From observations, one can also constrain the "shape of the Universe." A non-trivial cosmic topology [57–62] arises if the Universe is not simply connected. In the latter case, it can have disconnected components or be multi-connected, i.e., some spacetime points are identified. The closed compact (hypersphere), flat and open non-compact FLRW topologies are only three special cases among many other possibilities, including some where spatial sections are flat and compact (3-torus $\mathbb{T}^3$; e.g., [63]), flat and non-compact (some Clifford–Klein spaces [57, 64]) or with positive curvature (some Clifford–Klein spaces or, e.g., Poincaré dodecahedral space [65]).

Detecting topology is difficult because the dynamics is, in general, the same. For example, the hypertorus $\mathbb{T}^3$ is locally isomorphic to three-dimensional Euclidean space, so that spatial flat sections and the 3-torus share the same metric; the only change is in the boundary conditions. If the characteristic curvature scale of the topology is larger than the observed universe, then there is little or no hope to see any effect. However, if the observed patch is larger than physical space, one could observe multiple images of luminous sources in large-scale structures [66] and the CMB [67].

The impact of topology on the cosmic microwave background and its interplay with the inflationary mechanism have been studied extensively [65, 68–99]. A total density parameter close to the critical value $\Omega \sim 1$ implies that many topologies are undetectable, while others are already excluded. For some compact and semi-compact topologies, one can place bounds on their characteristic scale [99]. Although, so far, there is no evidence for a non-trivial topology and the scale of a compact topology is tightly constrained [100, 101], it may be important to keep an eye on this direction. A Universe with non-trivial topology can arise, for instance, via quantum creation in Wheeler–DeWitt quantum cosmology [63, 90, 102–104], in string theory [105, 106] or in quantum gravity and quantum cosmology models of "third quantization" (Sect. 10.2.4). The discovery of an imprint of a specific cosmic topology could be relevant in the big quest of a quantum theory of Nature, since it could justify, constrain or refine some of the models mentioned in this book.

2.6 An Obscure Big Picture

To summarize, the total density parameter measured today is

$$\Omega_0 = \Omega_{\mathrm{K}0} + \Omega_{\mathrm{r}0} + (\Omega_{\mathrm{b}0} + \Omega_{\mathrm{c}0}) + \Omega_{\Lambda 0}\,. \tag{2.129}$$

Using the estimate of the Hubble parameter h in (2.12), and neglecting radiation and curvature contributions (which amount to less than 1 % of the total), one ends up with the following picture:

$$\Omega_{\mathrm{b}0} \sim 4.8\,\%\,, \qquad \Omega_{\mathrm{c}0} \sim 26\,\%\,, \qquad \Omega_{\mathrm{m}0} \sim 31\,\%\,, \qquad \Omega_{\Lambda 0} \sim 69\,\%\,. \tag{2.130}$$

We do not have striking evidence in favour of any specific model of cold dark matter or dark energy over the others, so we could say that we know less than 5 % of our world! The first cosmological models did not have dark components at all, but observations forced themselves upon our conception, which was then changed to make room for new ingredients. As Figs. 2.9 and 2.10 illustrate, our picture of the universe has been evolving dramatically in the last fifty years. Science is a measure of our ignorance.

To the best of our knowledge, the concordance model still fits all data without the compelling need to invoke exotic physics such as supersymmetry, string theory or quantized gravity. In this sense, cosmology does not really need quantum gravity at large. However, certain ingredients create a sense of uneasiness in the researcher, mainly for theoretical reasons. The cosmological constant problem, both in its old version of Sect. 2.5.3 and in the new one (Why is $\Omega_{\Lambda 0}$ of the same order of magnitude as $\Omega_{\mathrm{m}0}$?) is one example and we will soon see others (the big-bang

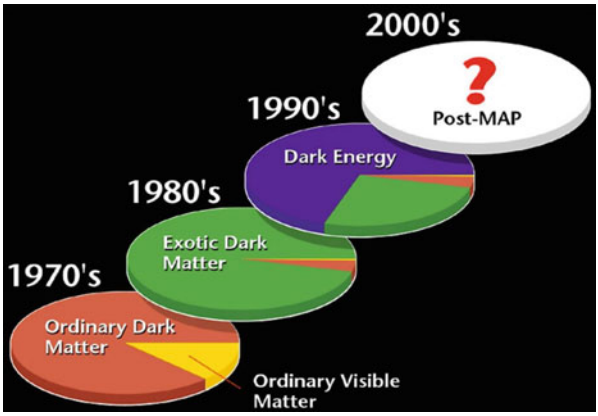

Fig. 2.9 Evolution of our knowledge of the content of the universe from the 1970s (Credit: NASA/WMAP Science Team)

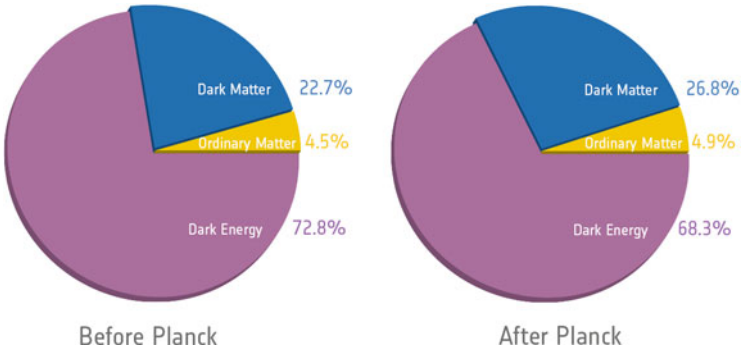

Fig. 2.10 Content of the universe as estimated by WMAP [12] (*left pie chart*) and PLANCK 2013 [107] (*right*) (©ESA and the Planck Collaboration [13])

problem and the inflation-related problems). So, in this other respect, quantum gravity might need cosmology. One duty of modern theoretical physics beyond the Standard Model is to be in agreement with observations, in particular cosmological. Suppose, for instance, one has a model of matter and gravity at hand which can explain a late stage of acceleration (this is a typical goal of phenomenology). One starts from the Friedmann equations or their analogue in, e.g., synchronous time, which is an unphysical parameter. Switching to expressions in redshift z such as (2.87) and (2.88), rescaling the energy densities $\rho_i \rightarrow \Omega_i$ and plugging the measured values Ω_{i0} for all the components inserted "by hand" (e.g., matter and radiation), one can follow the dynamical evolution from large redshift until today or to the future, and constrain the parameters of the model (in this example, those determining the dark energy density).

However, it is often difficult to falsify phenomenological models on the basis of constraints placed *a posteriori*. It would be greatly desirable to construct models with *predictive* power, i.e., with few or no free parameters, or such that its free parameters determine the cosmological observables only within certain intervals. Therefore, a second, tremendously challenging task of theoretical physics is to enhance its predictive power by asking the right questions on one hand (What are the physical observables? How can we formulate the cosmological constant and big-bang problems in a non-misleading, operational way?) and looking towards the right directions on the other hand: Does the model agree with observations? How are dark energy and inflation realized? Can we build an arsenal of smoking guns to favour one model against another?

2.7 Problems and Solutions

2.1 Age of the universe. Calculate the formula for the age of the universe in the presence of matter and a cosmological constant. Compare it with the estimate $t_0 \sim H_0^{-1}$ given in (2.13) (ignore error bars).

Solution From (2.81) and (2.88), it follows that

$$H^2 = \frac{\kappa^2}{3}\left(\rho_\mathrm{m} + \frac{\Lambda}{\kappa^2}\right) = H^2\left(\Omega_\mathrm{m} + \Omega_\Lambda\right) = H_0^2\left(1 - \Omega_{\mathrm{m}0} + \Omega_{\mathrm{m}0}a^{-3}\right) .$$

In the last step, we have used the fact that $\Omega_{\Lambda 0} = 1 - \Omega_{\mathrm{m}0}$. The above equation can be integrated from the beginning ($a(t_\mathrm{i}) = a_\mathrm{i}$) until today ($a_0 = 1$). Since $t_\mathrm{i} \ll t_0$, one then has $a_\mathrm{i} \approx 0$ and

$$\begin{aligned} t_0 &= \frac{1}{H_0}\int_0^1 \frac{\mathrm{d}a}{\sqrt{(1-\Omega_{\mathrm{m}0})a^2 + \Omega_{\mathrm{m}0}a^{-1}}} \\ &= \frac{1}{H_0}\frac{2}{3\sqrt{1-\Omega_{\mathrm{m}0}}}\ln\left(\frac{1+\sqrt{1-\Omega_{\mathrm{m}0}}}{\sqrt{\Omega_{\mathrm{m}0}}}\right) \\ &\approx 0.955 \times \frac{1}{H_0} \\ &\approx 13.79\,\mathrm{Gyr}\,, \end{aligned}$$

where we used (2.12), (2.13) and (2.99). This estimate is 96 % the crude one $t_0 \sim H_0^{-1}$ and is very close to (2.14). Adding also radiation does not change the numbers because the radiation-dominated era is only a small fraction of the present age.

2.2 Equality and decoupling. An important epoch in the history of the early universe is *decoupling*, when radiation last scattered with matter. Observations center this period at

$$z_\mathrm{dec} \approx 1091\,. \tag{2.131}$$

How old was the universe at z_dec and z_eq? Use the experimental estimate of the age of the universe today t_0 and ignore the errors.

Solution We must express the redshift z as a function of time t, and to do so we have to choose a profile $a(t)$. For redshifts $z \gtrsim z_{\rm eq}$, we can use (2.93):

$$z(t) + 1 = \frac{a_0}{a(t)} = \left(\frac{t_0}{t}\right)^p \qquad \Rightarrow \qquad t = \frac{t_0}{[z(t)+1]^{1/p}} \,. \tag{2.132}$$

The universe is dominated by dust and $p = 2/3$. For the age given in (2.14), $t_0 \approx 13.8\,\text{Gyr}$, one obtains

$$t_{\rm dec} \approx 3.83 \times 10^5\,\text{yr} \,. \tag{2.133}$$

At decoupling time, the universe was about 380,000 years old. Equation (2.91) is still an acceptable approximation near matter-radiation equality,

$$t_{\rm eq} \approx 7.0 \times 10^4\,\text{yr} \,. \tag{2.134}$$

2.3 Cosmological horizons 1. Describe the behaviour of the proper and comoving particle horizons for flat power-law cosmologies (2.93) with $0 < p < 1$ and a barotropic fluid (no cosmological constant).

Solution From the Friedmann equations, one can see that the Hubble parameter always decreases if $w > -1$:

$$\dot{H} = -\frac{3}{2}H^2(1+w) \,. \tag{2.135}$$

Therefore, the Hubble horizon always increases. In particular, for $w > -1/3$ ($0 < p < 1$) the particle horizon is well defined and follows the same evolution as R_H. From (2.95) and $t_{\rm i} = 0$,

$$R_{\rm p} = \frac{t}{1-p} = \frac{p}{1-p}\frac{1}{H} \,. \tag{2.136}$$

Also the comoving particle horizon increases with time,

$$\tau = \frac{R_{\rm p}}{a} = \frac{t^{1-p}}{1-p} = \frac{p}{1-p} r_H \,, \tag{2.137}$$

but at a lower rate.

2.4 Cosmological horizons 2. Determine the recession speed (in c units) of the particle horizon for power-law cosmologies (2.93) with $0 < p < 1$ and a barotropic fluid (no cosmological constant). Does the recession speed violate any principle of special or general relativity?

Solution From (2.136),

$$\dot{R}_{\rm p} = \frac{c}{1-p} > c\,. \tag{2.138}$$

This result does not violate special relativity, because the latter is valid only in local inertial frames and does not apply to relative speeds of distant objects. On the other hand, one requires that signals do not travel faster than light, but no signal is interchanged between us and the horizon.

2.5 Horizons and distances 1. Determine the size of the particle and Hubble horizons at $z_{\rm eq}$, $z_{\rm dec}$ and today for a matter-dominated universe. How much did the observable universe increase from decoupling to equality and from equality until today?

Solution At these redshifts, (2.91) is a very good approximation of the cosmic expansion. From (2.95) and (2.132), one has

$$z+1 = \left(\frac{H}{H_0}\right)^p \qquad \Rightarrow \qquad \frac{1}{H} = \frac{1}{H_0(z+1)^{1/p}}\,. \tag{2.139}$$

We know that

$$\frac{1}{H_0} \approx 3h^{-1}\,{\rm Gpc} \approx 4.42\,{\rm Gpc}\,. \tag{2.140}$$

Therefore, for $p = 2/3$ the size of the particle horizon is $R_{\rm p} = 2/H$ and

$$R_{\rm p}(z_{\rm eq}) \approx 45\,{\rm kpc}\,, \qquad R_{\rm p}(z_{\rm dec}) \approx 245\,{\rm kpc}\,, \qquad R_{\rm p}(0) \approx 8.8\,{\rm Gpc}\,.$$

The Hubble horizon H^{-1} is simply half the particle horizon. The growth rate of the horizons from redshift z_1 to redshift z_2 is

$$\frac{R_{\rm p}(z_2)}{R_{\rm p}(z_1)} = \frac{R_H(z_2)}{R_H(z_1)} = \left(\frac{1+z_1}{1+z_2}\right)^{3/2}\,, \tag{2.141}$$

so that

$$\frac{R_{\rm p}(z_{\rm dec})}{R_{\rm p}(z_{\rm eq})} \approx 5.5\,, \qquad \frac{R_{\rm p}(0)}{R_{\rm p}(z_{\rm dec})} \approx 36\times 10^3\,, \qquad \frac{R_{\rm p}(0)}{R_{\rm p}(z_{\rm eq})} \approx 2\times 10^5\,.$$

The comoving particle horizon is

$$\tau(z) = (1+z)R_{\rm p}(z) = \frac{1}{H_0}(z+1)^{1-\frac{1}{p}}\,. \tag{2.142}$$

It follows that $\tau_0 = R_{\rm p}(0)$, while

$$\tau_{\rm eq} \approx 152\,{\rm Mpc}\,, \qquad \tau_{\rm dec} \approx 268\,{\rm Mpc}\,.$$

The growth ratios are

$$\frac{\tau_{\rm dec}}{\tau_{\rm eq}} \approx 1.8\,, \qquad \frac{\tau_0}{\tau_{\rm dec}} \approx 33\,, \qquad \frac{\tau_0}{\tau_{\rm eq}} \approx 58\,.$$

2.6 Horizons and distances 2. Repeat the previous exercise for the ΛCDM model with radiation included. Find analytic expressions for the correction factors.

Solution A better estimate of particle horizons should also take radiation and the cosmological constant into account:

$$\begin{aligned}\tau(z) &= \int_0^{a(z)} \frac{{\rm d}a}{Ha^2} \\ &= \frac{1}{H_0}\int_0^{(1+z)^{-1}} \frac{{\rm d}a}{\sqrt{(1-\Omega_{\rm m0}-\Omega_{\rm r0})a^4 + \Omega_{\rm m0}a + \Omega_{\rm r0}}}\,.\end{aligned} \tag{2.143}$$

The integral can be done exactly in certain regimes. At high redshifts $10 < z < 10^4$, one can ignore the cosmological constant and obtain

$$\begin{aligned}\tau(z) &\simeq \frac{1}{H_0}\int_0^{(1+z)^{-1}} \frac{{\rm d}a}{\sqrt{\Omega_{\rm m0}a + \Omega_{\rm r0}}} \\ &= \tau_{\rm CDM}(z)\,\frac{\sqrt{\Omega_{\rm r0}(1+z)+\Omega_{\rm m0}} - \sqrt{\Omega_{\rm r0}(1+z)}}{\Omega_{\rm m0}}\,,\end{aligned} \tag{2.144}$$

where

$$\tau_{\rm CDM}(z) = \frac{2}{H_0\sqrt{1+z}}\,. \tag{2.145}$$

In particular, the correction factors with respect to those found in the previous exercise are

$$\tau_{\rm eq} \approx 0.89\,\tau_{\rm CDM,eq}\,, \qquad \tau_{\rm dec} \approx 1.18\,\tau_{\rm CDM,dec}\,. \tag{2.146}$$

As expected, the correction factors are close to 1.

At late times, dark energy is causing the recent expansion of the universe to be greater than in the past. Therefore, we expect to obtain a higher value for τ_0. In fact,

$$\begin{aligned}\tau(z) &= \frac{1}{H_0}\int_0^{(1+z)^{-1}} \frac{{\rm d}a}{\sqrt{(1-\Omega_{\rm m0})a^4 + \Omega_{\rm m0}a}} \\ &= \tau_{\rm CDM,0}\frac{1}{\sqrt{\Omega_{\rm m0}}}F\left[\frac{1}{6},\frac{1}{2};\frac{7}{6};-\frac{1-\Omega_{\rm m0}}{\Omega_{\rm m0}(1+z)^3}\right],\end{aligned} \tag{2.147}$$

where F is the *hypergeometric function*

$$F(a,b;c;x) := \sum_{n=0}^{\infty}\frac{\Gamma(a+n)\Gamma(b+n)}{\Gamma(a)\Gamma(b)}\frac{\Gamma(c)}{\Gamma(c+n)}\frac{x^n}{n!}\,. \tag{2.148}$$

Today, $\tau_0 \approx 1.63\,\tau_{\rm CDM,0}$. The effect, actually, turns out to be quite large because the universe has been accelerating for about half its age. Including all contributions (radiation, matter, Λ), (2.143) yields

$$\tau_0 \approx 1.61\,\tau_{\rm CDM,0}\,. \tag{2.149}$$

Using (2.143), we summarize the results in Table 2.1.

The growth ratios do not change much and are

$$\frac{\tau_{\rm dec}}{\tau_{\rm eq}} \approx 2.3\,, \qquad \frac{\tau_0}{\tau_{\rm dec}} \approx 45\,, \qquad \frac{\tau_0}{\tau_{\rm eq}} \approx 106\,, \tag{2.150}$$

Table 2.1 Comoving and proper particle horizons

z	τ	$R_{\rm p}$
$z_{\rm eq}$	134 Mpc	39 kpc
$z_{\rm dec}$	315 Mpc	289 kpc
0	14.2 Gpc	

and

$$\frac{R_{\rm p}(z_{\rm dec})}{R_{\rm p}(z_{\rm eq})} \approx 7.3\,, \qquad \frac{R_{\rm p}(0)}{R_{\rm p}(z_{\rm dec})} \approx 5\times 10^4\,, \qquad \frac{R_{\rm p}(0)}{R_{\rm p}(z_{\rm eq})} \approx 3.6\times 10^5\,. \tag{2.151}$$

From matter-radiation equality until today, the linear size of the causal patch (observable universe) has been increasing 360,000 times.

2.7 Distances. Determine the distance of luminous objects at redshift z. Write an approximate formula for $z \ll 1$. How far are sources at $z_{\rm dec}$ in a flat universe? And galaxies at $z = 0.2$?

Solution The comoving distance $\chi(t)$ of an object at redshift $z(t)$ from us is the distance light covered from time t until today. This is related to the particle horizon via the photon geodesic equation. In conformal time ($c = 1$),

$$0 = {\rm d}s^2 = a^2(\tau)\left(-{\rm d}\tau^2 + \frac{{\rm d}r^2}{1-{\rm K}r^2}\right), \tag{2.152}$$

where r is the spatial coordinate interval. Taking the square root and integrating,

$$\int_\tau^{\tau_0} {\rm d}\tau' = \int_0^\chi \frac{{\rm d}r}{\sqrt{1-{\rm K}r^2}}\,. \tag{2.153}$$

Inverting with respect to χ,

$$\chi(\tau) = \begin{cases} |{\rm K}|^{-1/2}\sinh\left[|{\rm K}|^{1/2}(\tau_0-\tau)\right], & {\rm K}<0 \\ \tau_0-\tau\,, & {\rm K}=0 \\ {\rm K}^{-1/2}\sin\left[{\rm K}^{1/2}(\tau_0-\tau)\right], & {\rm K}>0 \end{cases}. \tag{2.154}$$

In a flat or closed universe, signals emitted inside the particle horizon could not have travelled a distance greater than the radius of the horizon today.

For high redshifts, the comoving distance in a *flat* universe is well approximated by the particle horizon today. For instance, at $z = z_{\rm dec}$ the comoving horizon is one order of magnitude smaller that the horizon today τ_0 (see (2.150)) and the comoving distance of the $z = z_{\rm dec}$ surface (*last-scattering surface*) is

$$\chi(z_{\rm dec}) \simeq \tau_0 \approx 9.6h^{-1}\,{\rm Gpc} \approx 14.2\,{\rm Gpc}\,, \tag{2.155}$$

where we presented the result also in the standard form with the h factor reinstated.

The proper distance

$$d(z) := a(z)\chi(z) = (1+z)\,\chi(z) \tag{2.156}$$

$$= \frac{R_{\rm p}(0)}{1+z} - R_{\rm p}(z) \tag{2.157}$$

is always smaller than χ. We will see in Chap. 4 that $z_{\rm dec}$ corresponds to the time when the CMB was originated. Since the CMB is isotropic only in the comoving coordinate frame,[7] statements about the "distance" of the last scattering surface implicitly refer to the comoving distance $\chi(z)$.

At small redshift, curvature effects can be neglected. The proper and comoving distances are about the same and one can expand (2.157) to get

$$d(z) = a_0\chi(z) + O(z^2) = -\frac{c}{H_0 a_0}\partial_z a(z)\big|_{z=0} z + O(z^2)$$

$$= \frac{cz}{H_0} + O(z^2) \approx 3z\,h^{-1}\,\text{Gpc}\,. \tag{2.158}$$

Objects at $z = 0.2$ are $600\,h^{-1}$ Mpc away from us. The 2dFGRS survey covers redshifts $z \lesssim 0.3$, so that the largest redshift observed by the survey corresponds to a distance of about 1.3 Gpc. The SDSS main galaxy sample contains galaxies with $z \lesssim 0.4$ and quasars as far as $z \sim 5$.

Another distance of great interest in astrophysics is the *luminosity distance*, which can be expressed either via the absolute magnitude $M_{\rm abs}$ of an object and its apparent magnitude $M_{\rm app}$ or via the luminosity L (in Watts) and the energy flux $\mathcal{F}$ (Watts per area):

$$d_L := 10^{\frac{M_{\rm app}-M_{\rm abs}}{5}-5}\,\text{Mpc} = \sqrt{\frac{L}{4\pi\mathcal{F}}}\,. \tag{2.159}$$

The luminosity of certain objects such as type I supernovæ is known. For these "standard candles," the luminosity distance can be determined with a certain accuracy. In these cases, $d_L = \chi(\tau) \simeq \tau_0 - \tau$ and, via (2.156), one can extract valuable information on the expansion properties of the universe.

2.8 Thermal history of the universe. Determine the temperature of radiation at $z_{\rm eq}$, $z_{\rm dec}$ and today. Calculate the age and the order of magnitude of

(continued)

[7] Sometimes, this frame preference is perceived as a contradiction of general relativity. However, global coordinate frames may be defined once we fix our metric. The observed CMB frame is a solution of Einstein's equations.

redshift corresponding to $T \sim 1\,\mathrm{MeV}$ and $T \sim 0.1\mathrm{MeV}$. Assume $g_* = 1$ and round up the numbers from below, since $g_* > 1$.

Solution From (2.103) and (2.104),

$$T_{\mathrm{eq}} \approx 1\,\mathrm{eV} \approx 10^4\,\mathrm{K}\,, \tag{2.160}$$

$$T_{\mathrm{dec}} \approx 0.3\,\mathrm{eV} \approx 3 \times 10^3\,\mathrm{K}\,, \tag{2.161}$$

$$T_0 \approx 3 \times 10^{-4}\,\mathrm{eV} \approx 3\,\mathrm{K}\,. \tag{2.162}$$

More precise numbers can be obtained by inserting realistic values for g_* [108]. In particular, (2.162) agrees with the measured temperature (2.1) of the microwave background.

$T \sim 1\,\mathrm{MeV} \sim 10^{10}\,\mathrm{K}$ is the typical binding energy of nuclei. When the temperature of the universe is lower than that, atomic nuclei are being synthesized. From (2.103) and (2.106) at high redshift ($z \sim 10^4 T\,\mathrm{eV}^{-1}$), we get

$$t \approx 2\,\mathrm{s}\,, \qquad z \sim 10^{10}\,. \tag{2.163}$$

However, the inverse process also occurs and nuclei are destroyed until the universe cools down enough. One can show that ^{4}He nuclei begin to form at about $T \sim 0.1$ MeV. This temperature roughly marks the onset of the epoch known as big-bang nucleosynthesis:

$$t_{\mathrm{BBN}} \approx 200\,\mathrm{s}\,, \qquad z_{\mathrm{BBN}} \sim 10^9\,. \tag{2.164}$$

This era begins three minutes after the big bang and lasts about 17 minutes, after which the nuclear fusion reaction rate drops off ($T \sim 20$–$50\,\mathrm{keV}$). Measurements of light elements have confirmed these calculations. Nucleosynthesis has been taking place again in the core of stars since their formation, 100 million years after the big bang.

We summarize the thermal history of the universe in Table 2.2. The particle horizon before equivalence is found from (2.139) and (2.105),

$$R_{\mathrm{p}} = \frac{1}{H} = \frac{1}{H_0 \Omega_{\mathrm{r0}}^{1/2} (1+z)^2} \approx 6 \times 10^8 z^{-2}\,\mathrm{kpc} \approx 2 \times 10^{25} z^{-2}\,\mathrm{km}\,, \tag{2.165}$$

which also correctly reproduces the large-z asymptotic limit of (2.143).

The reader should not take these values too seriously. Depending on both the available experimental data and the details of the high-energy particle physics involved during the early stages, the big-bang timeline can change from time to time, and from book to book. However, it is still remarkable that we have been able

Table 2.2 Simplified thermal history of the universe from BBN until today. The first line corresponds to the highest energy probed in ground-based laboratories, at the Large Hadron Collider (LHC) [109]. The values of this table should be taken only as indicative

T (K)	T (eV)	t	z	R_p	Event
10^{16}	10^{12}	10^{-12} s	10^{16}	0.2 mm	Highest energy probed in laboratory (LHC).
10^{10}	10^{5}	2 s	10^{10}	10^{5} km	Formation and destruction of nuclei begins.
10^{9}	10^{4}	200 s	10^{9}	10^{7} km	**Nucleosynthesis** of light ions.
10^{8}	3×10^{3}	20 min	10^{8}	10^{9} km	Big-bang nucleosynthesis ends.
10^{4}	1	7.0×10^{4} yr	3400	39 kpc	Radiation-matter **equality**. Matter domination begins.
3000	0.3	3.8×10^{5} yr	1090	289 kpc	**Decoupling** of matter and radiation. CMB forms. Atoms form.
100	10^{-2}	10^{8} yr	25	110 Mpc	First stars.
3	3×10^{-4}	14×10^{9} yr	0	14.2 Gpc	Today.

to reconstruct the history of the early universe in such a detail from a handful of formulæ. We collect them here again in an approximated fashion, for a radiation-dominated universe:

$$T_\mathrm{K} \sim 10^4 \left(\frac{T_\mathrm{eV}}{1\,\mathrm{eV}}\right) \mathrm{K}\,, \qquad t \sim \left(\frac{10^6\,\mathrm{eV}}{T_\mathrm{eV}}\right)^2 \mathrm{s}\,,$$
$$z \sim 10^4 \left(\frac{T_\mathrm{eV}}{1\,\mathrm{eV}}\right), \qquad R_\mathrm{p} \sim 10^{25} z^{-2}\,\mathrm{km}\,.$$

2.9 Accelerating universe. Consider a $D = 4$ flat universe filled only with a barotropic fluid. Discuss the meaning and behaviour of the parameter

$$\epsilon \coloneqq -\frac{\mathrm{d}\ln H}{\mathrm{d}\ln a} = -\frac{\dot{H}}{H^2} = 1 - \frac{\ddot{a}}{aH^2}\,. \tag{2.166}$$

Can an accelerating universe be dominated by matter or radiation?

Solution Equation (2.166) is the definition of the so called *first slow-roll parameter*, and is nothing but the recession speed of the particle horizon:

$$\epsilon = \dot{R}_H \,. \tag{2.167}$$

From (2.135), one sees that $\epsilon = 0$ for $w = -1$ (cosmological constant, de Sitter expansion), $\epsilon > 0$ for $w > -1$, and $\epsilon < 0$ for $w < -1$. In the latter case the Hubble parameter (horizon) increases (respectively, decreases) with time, a situation called *super-acceleration*. Moreover, (2.127) and (2.166) yield the additional constraint $\epsilon > 1$ when $w > -1/3$. Summarizing,

$$\epsilon < 0 \qquad \text{if} \qquad w < -1 \,, \tag{2.168a}$$

$$\epsilon = 0 \qquad \text{if} \qquad w = -1 \,, \tag{2.168b}$$

$$0 < \epsilon < 1 \qquad \text{if} \qquad -1 < w < -\tfrac{1}{3} \,, \tag{2.168c}$$

$$\epsilon > 1 \qquad \text{if} \qquad w > -\tfrac{1}{3} \,. \tag{2.168d}$$

In particular, we have acceleration only if $\epsilon < 1$ and power-law cosmologies (2.93) with $0 < p = 1/\epsilon < 1$ cannot accelerate. Equations (2.168b) and (2.168c) define a period of *inflation* ($\ddot{a} > 0$), while (2.168a) corresponds to *super-inflation* ($\dot{H} > 0$).

2.10 Exact solutions: H = const. Consider a D-dimensional universe with $\Lambda = 0$ filled with a scalar field with potential V. Find the exact solutions of the equations of motion for a constant Hubble parameter, listing $a(t)$, $\epsilon(t)$, $\phi(t)$ and $V(\phi)$. Recast the solutions in conformal time.

Solution The Friedmann and continuity equations are

$$\left(\frac{D}{2} - 1\right) H^2 = \frac{\kappa^2}{D-1} \left(\frac{\dot{\phi}^2}{2} + V\right) - \frac{\mathrm{K}}{a^2} \,, \tag{2.169}$$

$$H^2 + \dot{H} = \frac{\kappa^2}{D-1} \left[\frac{2}{D-2} V - \dot{\phi}^2\right] \,, \tag{2.170}$$

$$0 = \ddot{\phi} + (D-1) H \dot{\phi} + V_{,\phi} \,. \tag{2.171}$$

For a constant Hubble parameter $H(t) = H$,

$$a(t) = \mathrm{e}^{Ht} \,, \qquad \epsilon(t) = 0 \,. \tag{2.172}$$

In a flat universe, the exact solution of the Friedmann and scalar equations is just a cosmological constant (de Sitter spacetime),

$$\phi(t) = \phi_0\,, \qquad V(\phi) = \frac{(D-1)(D-2)H^2}{2\kappa^2}\,, \qquad \mathrm{K} = 0\,. \tag{2.173}$$

The Friedmann equations show that there is no solution if $\mathrm{K} = -1$, while there is one for a closed universe, but only in $D = 4$:

$$\phi_\pm(t) = \pm\sqrt{\frac{2}{\kappa^2 H^2}}\mathrm{e}^{-Ht}\,, \qquad \mathrm{K} = 1\,,$$

while the continuity equation fixes the potential:

$$V(\phi) = \frac{3H^2}{\kappa^2} + H^2\phi^2\,. \tag{2.174}$$

This solution is *not* de Sitter because spatial sections are not flat. (We recall that the $H = $ const cosmology corresponds mathematically to de Sitter spacetime only if spatial sections are flat. In that case, the de Sitter hyperboloid is only half covered by FLRW coordinates.) The scalar field $\phi_\pm$ rolls down its potential from $t = -\infty$ and climbs it again after passing the global minimum. The solution is actually unique, since cosmological equations of motion are invariant under *time reversal*,

$$t \to -t\,, \tag{2.175}$$

and the direction of the rolling in a symmetric potential does not matter.

We can recast proper-time solutions into expressions in conformal time by inverting $\tau(t)$. For an $H = $ const background,

$$\tau = \int \mathrm{d}t\,\mathrm{e}^{-Ht} = -\frac{\mathrm{e}^{-Ht}}{H}\,, \tag{2.176}$$

so that

$$t = -\frac{\ln(-H\tau)}{H}\,. \tag{2.177}$$

Notice that τ runs from $-\infty$ to 0, so that the above expression is well defined. The geometric background in τ is

$$a(\tau) = \frac{1}{H|\tau|}\,, \qquad \mathcal{H}(\tau) := \frac{a'}{a} = aH = \frac{1}{|\tau|}\,, \tag{2.178}$$

where a prime denotes differentiation with respect to τ. The solution in the closed universe is linear in τ,

$$\phi(\tau) = \phi_0 |\tau| \,. \tag{2.179}$$

2.11 Exact solutions: power-law expansion. Repeat the same calculations of the previous exercise for a power-law expansion, $a \propto t^p$, where $p > 0$.

Solution In this case,

$$a(t) = \left(\frac{t}{\bar{t}}\right)^p \,, \qquad H(t) = \frac{p}{t} \,, \qquad \epsilon(t) = \frac{1}{p} \,, \tag{2.180}$$

where $\bar{t}$ is some reference time. Trying the profile $\phi(t) = (\phi_0/q)t^q$ in the (sum of the) Friedmann equations, one finds that it must be $q = 0$. This suggests to consider the limit $q \to 0$, which is a logarithmic profile:

$$\phi(t) = \phi_0 \ln(t/\bar{t}) \,. \tag{2.181}$$

From now on, $\bar{t} = 1$. This gives the exponential potential [110–113]

$$V(\phi) = \frac{(D-1)p - 1}{2} \phi_0^2 \, \mathrm{e}^{-2\phi/\phi_0} \,. \tag{2.182}$$

If the universe is flat, then

$$\phi_0 = \pm \sqrt{\frac{(D-2)p}{\kappa^2}} \,, \qquad \mathrm{K} = 0 \,, \tag{2.183}$$

while for a curved universe only the case $p = 1$ is a solution:

$$\phi_0 = \pm \sqrt{\frac{D - 2 + 2\mathrm{K}}{\kappa^2}} \,, \qquad p = 1 \,. \tag{2.184}$$

This solution is real only if $D > 2(1 - \mathrm{K})$. Therefore, it is always valid for a closed universe, while for an open universe it exists only in $D > 4$.

For a power-law expansion, conformal time is

$$\tau = \int \mathrm{d}t \, t^{-p} = \frac{t^{1-p}}{1-p} \,, \qquad p \neq 1 \,, \tag{2.185}$$

which is positive if $p < 1$. Inverting this expression,

$$t = [(1-p)\tau]^{\frac{1}{1-p}} . \tag{2.186}$$

The solution with $\kappa = 0$ is

$$a(\tau) = \left(\frac{\tau}{\tau_0}\right)^{\frac{p}{1-p}} , \qquad \mathcal{H}(\tau) = \frac{p}{1-p}\frac{1}{\tau} , \qquad \phi(\tau) = \phi_0 \ln \tau , \tag{2.187}$$

while for $p = 1$

$$\tau = \int \frac{\mathrm{d}t}{t} = \ln t , \tag{2.188}$$

and the solution is

$$a(\tau) = \mathrm{e}^{\tau} , \qquad \mathcal{H}(\tau) = 1 , \qquad \phi(\tau) = \phi_0 \tau . \tag{2.189}$$

References

1. S. Cole et al. [The 2dFGRS Collaboration], The 2dF Galaxy Redshift Survey: power-spectrum analysis of the final dataset and cosmological implications. Mon. Not. R. Astron. Soc. **362**, 505 (2005). [arXiv:astro-ph/0501174]
2. http://www.aao.gov.au/local/www/6df
3. D. Heath Jones et al. [The 6dFGS Collaboration], The 6dF Galaxy Survey: final redshift release (DR3) and southern large-scale structures. Mon. Not. R. Astron. Soc. **399**, 683 (2009). [arXiv:0903.5451]
4. http://www.sdss3.org, http://classic.sdss.org, http://www.youtube.com/watch?v=08LBltePDZw
5. C.P. Ahn et al. [SDSS Collaboration], The tenth data release of the Sloan Digital Sky Survey: first spectroscopic data from the SDSS-III Apache Point Observatory Galactic Evolution Experiment. Astrophy. J. Suppl. **211**, 17 (2014). [arXiv:1307.7735]
6. M. Betoule et al., Improved photometric calibration of the SNLS and the SDSS supernova surveys. Astron. Astrophys. **552**, A124 (2013). [arXiv:1212.4864]
7. M. Betoule et al. [SDSS Collaboration], Improved cosmological constraints from a joint analysis of the SDSS-II and SNLS supernova samples. Astron. Astrophys. **568**, A22 (2014). [arXiv:1401.4064]
8. "2dfdtfe" by Willem Schaap – http://en.wikipedia.org/wiki/Sloan_Great_Wall. Licensed under Creative Commons Attribution-Share Alike 3.0 via Wikimedia Commons – http://commons.wikimedia.org/wiki/File:2dfdtfe.gif#mediaviewer/File:2dfdtfe.gif
9. http://www2.aao.gov.au/~TDFgg/Public/Pics/2dFzcone.jpg
10. http://map.gsfc.nasa.gov
11. C.L. Bennett et al. [WMAP Collaboration], Nine-year Wilkinson Microwave Anisotropy Probe (WMAP) observations: final maps and results. Astrophys. J. Suppl. **208**, 20 (2013). [arXiv:1212.5225]

12. G. Hinshaw et al. [WMAP Collaboration], Nine-year Wilkinson Microwave Anisotropy Probe (WMAP) observations: cosmological parameter results. Astrophys. J. Suppl. **208**, 19 (2013). [arXiv:1212.5226]
13. http://www.esa.int/Our_Activities/Space_Science/Planck
14. P.A.R. Ade et al. [Planck Collaboration], Planck 2015 results. XIII. Cosmological parameters. Astron. Astrophys. **594**, A13 (2016). [arXiv:1502.01589]
15. J.C. Mather, D.J. Fixsen, R.A. Shafer, C. Mosier, D.T. Wilkinson, Calibrator design for the COBE Far Infrared Absolute Spectrophotometer (FIRAS). Astrophys. J. **512**, 511 (1999). [arXiv:astro-ph/9810373]
16. D.J. Fixsen, The temperature of the cosmic microwave background. Astrophys. J. **707**, 916 (2009). [arXiv:0911.1955]
17. R.P. Kirshner, Hubble's diagram and cosmic expansion. Proc. Natl. Acad. Sci. **101**, 8 (2004)
18. A.G. Riess et al. [Supernova Search Team Collaboration], Observational evidence from supernovae for an accelerating universe and a cosmological constant. Astron. J. **116**, 1009 (1998). [arXiv:astro-ph/9805201]
19. J.L. Tonry et al. [Supernova Search Team Collaboration], Cosmological results from high-z supernovæ. Astrophys. J. **594**, 1 (2003). [arXiv:astro-ph/0305008]
20. R.A. Knop et al. [Supernova Cosmology Project Collaboration], New constraints on Ω_m, Ω_λ, and w from an independent set of eleven high-redshift supernovae observed with HST. Astrophys. J. **598**, 102 (2003). [arXiv:astro-ph/0309368]
21. A.G. Riess et al. [Supernova Search Team Collaboration], Type Ia supernova discoveries at $z > 1$ from the Hubble Space Telescope: evidence for past deceleration and constraints on dark energy evolution. Astrophys. J. **607**, 665 (2004). [arXiv:astro-ph/0402512]
22. W.M. Wood-Vasey et al. [ESSENCE Collaboration], Observational constraints on the nature of the dark energy: first cosmological results from the ESSENCE supernova survey. Astrophys. J. **666**, 694 (2007). [arXiv:astro-ph/0701041]
23. T.M. Davis et al., Scrutinizing exotic cosmological models using ESSENCE supernova data combined with other cosmological probes. Astrophys. J. **666**, 716 (2007). [arXiv:astro-ph/0701510]
24. W. Rindler, Visual horizons in world-models. Mon. Not. R. Astron. Soc. **116**, 662 (1956)
25. A. Einstein, Hamiltonsches Prinzip und allgemeine Relativitätstheorie. Sitz.-ber. Kgl. Preuss. Akad. Wiss. **1916**, 1111 (1916)
26. J.W. York, Role of conformal three-geometry in the dynamics of gravitation. Phys. Rev. Lett. **28**, 1082 (1972)
27. G.W. Gibbons, S.W. Hawking, Action integrals and partition functions in quantum gravity. Phys. Rev. D **15**, 2752 (1977)
28. S.W. Hawking, G.F.R. Ellis, *The Large Scale Structure of Space-Time* (Cambridge University Press, Cambridge, 1973)
29. S.W. Hawking, Perturbations of an expanding universe. Astrophys. J. **145**, 544 (1966)
30. G.F.R. Ellis, Relativistic cosmology, in *General Relativity and Cosmology, Proceedings of the XLVII Enrico Fermi Summer School*, ed. by R.K. Sachs (Academic Press, New York, 1971)
31. G.F.R. Ellis, M. Bruni, Covariant and gauge-invariant approach to cosmological density fluctuations. Phys. Rev. D **40**, 1804 (1989)
32. M.S. Madsen, Scalar fields in curved spacetimes. Class. Quantum Grav. **5**, 627 (1988)
33. S. Weinberg, *Gravitation and Cosmology* (Wiley, New York, 1972)
34. S. Colafrancesco, Dark matter in modern cosmology. AIP Conf. Proc. **1206**, 5 (2010). [arXiv:1004.3869]
35. Z. Ahmed et al. [CDMS-II Collaboration], Results from a low-energy analysis of the CDMS II Germanium data. Phys. Rev. Lett. **106**, 131302 (2011). [arXiv:1011.2482]
36. S. Galli, F. Iocco, G. Bertone, A. Melchiorri, CMB constraints on dark matter models with large annihilation cross-section. Phys. Rev. D **80**, 023505 (2009). [arXiv:0905.0003]
37. W. de Sitter, Einstein's theory of gravitation and its astronomical consequences. Third paper. Mon. Not. R. Astron. Soc. **78**, 3 (1917)

38. R. Utiyama, B.S. DeWitt, Renormalization of a classical gravitational field interacting with quantized matter fields. J. Math. Phys. **3**, 608 (1962)
39. T.P. Singh, T. Padmanabhan, Notes on semiclassical gravity. Ann. Phys. (N.Y.) **196**, 296 (1989)
40. Ya.B. Zel'dovich, The cosmological constant and the theory of elementary particles. Sov. Phys. Usp. **11**, 381 (1968)
41. Ya.B. Zel'dovitch, I.D. Novikov, *Relativistic Astrophysics*, vol. 1 (University of Chicago Press, Chicago, 1971)
42. S. Perlmutter et al. [The Supernova Cosmology Project], Discovery of a supernova explosion at half the age of the universe and its cosmological implications. Nature **391**, 51 (1998). [arXiv:astro-ph/9712212]
43. S. Perlmutter et al. [The Supernova Cosmology Project], Measurements of Ω and Λ from 42 high-redshift supernovæ. Astrophys. J. **517**, 565 (1999). [arXiv:astro-ph/9812133]
44. D.J. Eisenstein et al. [SDSS Collaboration], Detection of the baryon acoustic peak in the large-scale correlation function of SDSS luminous red galaxies. Astrophys. J. **633**, 560 (2005). [arXiv:astro-ph/0501171]
45. W.J. Percival et al. [SDSS Collaboration], Baryon acoustic oscillations in the Sloan Digital Sky Survey Data Release 7 galaxy sample. Mon. Not. R. Astron. Soc. **401**, 2148 (2010). [arXiv:0907.1660]
46. N.G. Busca et al., Baryon acoustic oscillations in the Ly-α forest of BOSS quasars. Astron. Astrophys. **552**, A96 (2013). [arXiv:1211.2616]
47. L. Anderson et al. [BOSS Collaboration], The clustering of galaxies in the SDSS-III Baryon Oscillation Spectroscopic Survey: baryon acoustic oscillations in the Data Release 10 and 11 galaxy samples. Mon. Not. R. Astron. Soc. **441**, 24 (2014). [arXiv:1312.4877]
48. A.J. Ross, L. Samushia, C. Howlett, W.J. Percival, A. Burden M. Manera, The clustering of the SDSS DR7 main galaxy sample I: a 4 per cent distance measure at $z = 0.15$. Mon. Not. R. Astron. Soc. **449**, 835 (2015). [arXiv:1409.3242]
49. M. Tegmark et al. [SDSS Collaboration], Cosmological constraints from the SDSS luminous red galaxies. Phys. Rev. D **74**, 123507 (2006). [arXiv:astro-ph/0608632]
50. L.-M. Wang, P.J. Steinhardt, Cluster abundance constraints on quintessence models. Astrophys. J. **508**, 483 (1998). [arXiv:astro-ph/9804015]
51. S. Tsujikawa, A. De Felice, J. Alcaniz, Testing for dynamical dark energy models with redshift-space distortions. JCAP **1301**, 030 (2013). [arXiv:1210.4239]
52. M. Chevallier, D. Polarski, Accelerating universes with scaling dark matter. Int. J. Mod. Phys. D **10**, 213 (2001). [arXiv:gr-qc/0009008]
53. E.V. Linder, Exploring the expansion history of the universe. Phys. Rev. Lett. **90**, 091301 (2003). [arXiv:astro-ph/0208512]
54. T. Padmanabhan, H. Padmanabhan, Cosmological constant from the emergent gravity perspective. Int. J. Mod. Phys. D **23**, 1430011 (2014). [arXiv:1404.2284]
55. A. Mazumdar, The origin of dark matter, matter-anti-matter asymmetry, and inflation. arXiv:1106.5408
56. A. Melchiorri, L. Pagano, S. Pandolfi, When did cosmic acceleration start? Phys. Rev. D **76**, 041301 (2007). [arXiv:0706.1314]
57. G.F.R. Ellis, Topology and cosmology. Gen. Relat. Grav. **2**, 7 (1971)
58. M. Lachièze-Rey, J.-P. Luminet, Cosmic topology. Phys. Rep. **254**, 135 (1995). [arXiv:gr-qc/9605010]
59. G.D. Starkman, Topology and cosmology. Class. Quantum Grav. **15**, 2529 (1998)
60. J.-P. Luminet, B.F. Roukema, Topology of the universe: theory and observation, in *Proceedings of the NATO Advanced Study Institute on Theoretical and Observational Cosmology*, ed. by M. Lachièze-Rey (Kluwer, Dordrecht, 1999); NATO Sci. Ser. C **541**, 117 (1999). [arXiv:astro-ph/9901364]
61. J.J. Levin, Topology and the cosmic microwave background. Phys. Rep. **365**, 251 (2002). [arXiv:gr-qc/0108043]

62. J.-P. Luminet, Cosmic topology: twenty years after. Grav. Cosmol. **20**, 15 (2014). [arXiv:1310.1245]
63. Ya.B. Zeldovich, A.A. Starobinsky, Quantum creation of a universe in a nontrivial topology. Sov. Astron. Lett. **10**, 135 (1984)
64. B.S. DeWitt, C.F. Hart, C.J. Isham, Topology and quantum field theory. Physica A **96**, 197 (1979)
65. J.-P. Luminet, J. Weeks, A. Riazuelo, R. Lehoucq, J.-P. Uzan, Dodecahedral space topology as an explanation for weak wide-angle temperature correlations in the cosmic microwave background. Nature **425**, 593 (2003). [arXiv:astro-ph/0310253]
66. E. Gausmann, R. Lehoucq, J.-P. Luminet, J.-P. Uzan, J. Weeks, Topological lensing in spherical spaces. Class. Quantum Grav. **18**, 5155 (2001). [arXiv:gr-qc/0106033]
67. R. Lehoucq, J. Weeks, J.-P. Uzan, E. Gausmann, J.-P. Luminet, Eigenmodes of three-dimensional spherical spaces and their application to cosmology. Class. Quantum Grav. **19**, 4683 (2002). [arXiv:gr-qc/0205009]
68. D.D. Sokolov, V.F. Shvartsman, An estimate of the size of the universe from a topological point of view. Zh. Eksp. Teor. Fiz. **66**, 412 (1974) [Sov. Phys. JETP **39**, 196 (1975)]
69. D.D. Sokolov, A.A. Starobinsky, Globally inhomogeneous "spliced" universes. Sov. Astron. **19**, 629 (1976)
70. N.J. Cornish, D.N. Spergel, G.D. Starkman, Does chaotic mixing facilitate $\Omega < 1$ inflation? Phys. Rev. Lett. **77**, 215 (1996). [arXiv:astro-ph/9601034]
71. J.J. Levin, E. Scannapieco, J. Silk, The topology of the universe: the biggest manifold of them all. Class. Quantum Grav. **15**, 2689 (1998). [arXiv:gr-qc/9803026]
72. G.I. Gomero, A.F.F. Teixeira, M.J. Rebouças, A. Bernui, Spikes in cosmic crystallography. Int. J. Mod. Phys. D **11**, 869 (2002). [arXiv:gr-qc/9811038]
73. J.R. Bond, D. Pogosian, T. Souradeep, CMB anisotropy in compact hyperbolic universes. 1. Computing correlation functions. Phys. Rev. D **62**, 043005 (2000). [arXiv:astro-ph/9912124]
74. J.R. Bond, D. Pogosian, T. Souradeep, CMB anisotropy in compact hyperbolic universes. 2. COBE maps and limits. Phys. Rev. D **62**, 043006 (2000). [arXiv:astro-ph/9912144]
75. J. Barrow, H. Kodama, The isotropy of compact universes. Class. Quantum Grav. **18**, 1753 (2001). [arXiv:gr-qc/0012075]
76. G.I. Gomero, M.J. Rebouças, R.K. Tavakol, Detectability of cosmic topology in almost flat universes. Class. Quantum Grav. **18**, 4461 (2001). [arXiv:gr-qc/0105002]
77. J.D. Barrow, H. Kodama, All universes great and small. Int. J. Mod. Phys. D **10**, 785 (2001). [arXiv:gr-qc/0105049]
78. G.I. Gomero, M.J. Rebouças, R.K. Tavakol, Are small hyperbolic universes observationally detectable? Class. Quantum Grav. **18**, L145 (2001). [arXiv:gr-qc/0106044]
79. G.I. Gomero, M.J. Rebouças, Detectability of cosmic topology in flat universes. Phys. Lett. A **311**, 319 (2003). [arXiv:gr-qc/0202094]
80. J. Weeks, R. Lehoucq, J.-P. Uzan, Detecting topology in a nearly flat spherical universe. Class. Quantum Grav. **20**, 1529 (2003). [arXiv:astro-ph/0209389]
81. G.I. Gomero, M.J. Rebouças, R. Tavakol, Limits on the detectability of cosmic topology in hyperbolic universes. Int. J. Mod. Phys. A **17**, 4261 (2002). [arXiv:gr-qc/0210016]
82. J.R. Weeks, Detecting topology in a nearly flat hyperbolic universe. Mod. Phys. Lett. A **18**, 2099 (2003). [arXiv:astro-ph/0212006]
83. A. Riazuelo, J.-P. Uzan, R. Lehoucq, J. Weeks, Simulating cosmic microwave background maps in multi-connected spaces. Phys. Rev. D **69**, 103514 (2004). [arXiv:astro-ph/0212223]
84. A. de Oliveira-Costa, M. Tegmark, M. Zaldarriaga, A. Hamilton, The significance of the largest scale CMB fluctuations in WMAP. Phys. Rev. D **69**, 063516 (2004). [arXiv:astro-ph/0307282]
85. B. Mota, M.J. Rebouças, R. Tavakol, Constraints on the detectability of cosmic topology from observational uncertainties. Class. Quantum Grav. **20**, 4837 (2003). [arXiv:gr-qc/0308063]
86. B. Mota, G.I. Gomero, M.J. Rebouças, R. Tavakol, What do very nearly flat detectable cosmic topologies look like? Class. Quantum Grav. **21**, 3361 (2004). [arXiv:astro-ph/0309371]

87. N.J. Cornish, D.N. Spergel, G.D. Starkman, E. Komatsu, Constraining the topology of the universe. Phys. Rev. Lett. **92**, 201302 (2004). [arXiv:astro-ph/0310233]
88. A. Riazuelo, J. Weeks, J.-P. Uzan, R. Lehoucq, J.-P. Luminet, Cosmic microwave background anisotropies in multi-connected flat spaces. Phys. Rev. D **69**, 103518 (2004). [arXiv:astro-ph/0311314]
89. B.F. Roukema, B. Lew, M. Cechowska, A. Marecki, S. Bajtlik, A hint of Poincaré dodecahedral topology in the WMAP first year sky map. Astron. Astrophys. **423**, 821 (2004). [arXiv:astro-ph/0402608]
90. A.D. Linde, Creation of a compact topologically nontrivial inflationary universe. JCAP **0410**, 004 (2004). [arXiv:hep-th/0408164]
91. R. Aurich, S. Lustig, F. Steiner, CMB anisotropy of the Poincaré dodecahedron. Class. Quantum Grav. **22**, 2061 (2005). [arXiv:astro-ph/0412569]
92. B. Mota, M.J. Rebouças, R. Tavakol, The local shape of the universe in the inflationary limit. Int. J. Mod. Phys. A **20**, 2415 (2005). [arXiv:astro-ph/0503683]
93. R. Aurich, S. Lustig, F. Steiner, CMB anisotropy of spherical spaces. Class. Quantum Grav. **22**, 3443 (2005). [arXiv:astro-ph/0504656]
94. R. Aurich, S. Lustig, F. Steiner, The circles-in-the-sky signature for three spherical universes. Mon. Not. R. Astron. Soc. **369**, 240 (2006). [arXiv:astro-ph/0510847]
95. M. Kunz, N. Aghanim, L. Cayon, O. Forni, A. Riazuelo, J.-P. Uzan, Constraining topology in harmonic space. Phys. Rev. D **73**, 023511 (2006). [arXiv:astro-ph/0510164]
96. R. Aurich, H.S. Janzer, S. Lustig, F. Steiner, Do we live in a small universe? Class. Quantum Grav. **25**, 125006 (2008). [arXiv:0708.1420]
97. B. Mota, M.J. Rebouças, R. Tavakol, Circles-in-the-sky searches and observable cosmic topology in the inflationary limit. Phys. Rev. D **78**, 083521 (2008). [arXiv:0808.1572]
98. B. Mota, M.J. Rebouças, R. Tavakol, Circles-in-the-sky searches and observable cosmic topology in a flat universe. Phys. Rev. D **81**, 103516 (2010). [arXiv:1002.0834]
99. G. Aslanyan, A.V. Manohar, The topology and size of the universe from the cosmic microwave background. JCAP **1206**, 003 (2012). [arXiv:1104.0015]
100. P.A.R. Ade et al. [Planck Collaboration], Planck 2013 results. XXVI. Background geometry and topology of the Universe. Astron. Astrophys. **571**, A26 (2014). [arXiv:1303.5086]
101. P.A.R. Ade et al. [Planck Collaboration], Planck 2015 results. XVIII. Background geometry and topology of the Universe. Astron. Astrophys. **594**, A18 (2016). [arXiv:1502.01593]
102. Yu.P. Goncharov, A.A. Bytsenko, The supersymmetric Casimir effect and quantum creation of the universe with nontrivial topology. Phys. Lett. B **160**, 385 (1985)
103. Yu.P. Goncharov, A.A. Bytsenko, The supersymmetric Casimir effect and quantum creation of the universe with nontrivial topology (II). Phys. Lett. B **169**, 171 (1986)
104. Yu.P. Goncharov, A.A. Bytsenko, Casimir effect in supergravity theories and the quantum birth of the Universe with non-trivial topology. Class. Quantum Grav. **4**, 555 (1987)
105. R.H. Brandenberger, C. Vafa, Superstrings in the early universe. Nucl. Phys. B **316**, 391 (1989)
106. B. McInnes, Inflation, large branes, and the shape of space. Nucl. Phys. B **709**, 213 (2005). [arXiv:hep-th/0410115]
107. P.A.R. Ade et al. [Planck Collaboration], Planck 2013 results. XVI. Cosmological parameters. Astron. Astrophys. **571**, A16 (2014). [arXiv:1303.5076]
108. D.H. Lyth, A.R. Liddle, *The Primordial Density Perturbation* (Cambridge University Press, Cambridge, 2009)
109. http://lhc.web.cern.ch/lhc
110. F. Lucchin, S. Matarrese, Power-law inflation. Phys. Rev. D **32**, 1316 (1985)
111. J.J. Halliwell, Scalar fields in cosmology with an exponential potential. Phys. Lett. B **185**, 341 (1987)
112. J. Yokoyama, K.-i. Maeda, On the dynamics of the power law inflation due to an exponential potential. Phys. Lett. B **207**, 31 (1988)
113. Y. Kitada, K.-i. Maeda, Cosmic no-hair theorem in power-law inflation. Phys. Rev. D **45**, 1416 (1992)

http://www.springer.com/978-3-319-41125-5

Classical and Quantum Cosmology

Calcagni, G.

2017, XV, 843 p. 80 illus., 52 illus. in color., Hardcover
ISBN: 978-3-319-41125-5